

Exploring temporal and spatial variation of nitrous oxide flux using several years of peatland forest automatic chamber data

Helena Rautakoski¹, Mika Korhonen¹, Jarmo Mäkelä², Markku Koskinen³, Kari Minkkinen⁴, Mika Aurela¹, Paavo Ojanen^{4,5}, Annalea Lohila^{1,6*}

¹Finnish Meteorological Institute, P.O. Box 503, FI-00101 Helsinki, Finland

²Advanced Computing Facility, CSC – IT Center for Science Ltd, P.O. Box 405, FI-02101 Espoo, Finland

³Department of Agriculture³Institute for Atmospheric and Earth System Research, University of Helsinki, Viikinkaari 9 Gustaf Hällströmin katu 2, P.O. Box 64, FI-0079000014 Helsinki, Finland

⁴Department of Forest Sciences, University of Helsinki, P.O. Box 27, FI-00014 Helsinki, Finland

⁵Natural Resources Institute Finland, Viikinkaari 4, FI-00790 Helsinki, Finland

⁶Institute for Atmospheric and Earth System Research, University of Helsinki, Gustaf Hällströmin katu 2, P.O. Box 64, FI-00014 Helsinki, Finland

Correspondence to: Helena Rautakoski (helena.rautakoski@fmi.fi)

Abstract: The urgent need to mitigate climate change has evoked a broad interest in better understanding and estimating nitrous oxide (N₂O) emissions from different ecosystems. Part of the uncertainty in N₂O emission estimates still comes from an inadequate understanding of the temporal and small-scale spatial variability of N₂O fluxes. Using 4.5 years of N₂O flux data collected in a drained peatland forest with six automated chambers, we explored temporal and small-scale spatial variability of N₂O fluxes. A Random forest with conditional inference trees was used to find immediate and ~~delayed~~ relationships between N₂O flux and environmental conditions across seasons and years ~~with different environmental conditions~~.

The ~~spatio-temporal~~ variation of the N₂O flux was large, ~~with the~~ daily mean N₂O flux ~~varying~~ varied between ~~-1044~~ and ~~+1760~~ $\mu\text{g N}_2\text{O m}^{-2} \text{h}^{-1}$ and annual N₂O budgets⁻¹. ~~Three of different~~ the six measurement chambers between ~~+60~~ and ~~+2110~~ $\text{mg N}_2\text{O m}^{-2} \text{y}^{-1}$. ~~had a maximum N₂O flux of less than 400 $\mu\text{g N}_2\text{O m}^{-2} \text{h}^{-1}$, while the fluxes in the other three chambers exceeded 1000 $\mu\text{g N}_2\text{O m}^{-2} \text{h}^{-1}$.~~ Spatial differences in ~~fluxes~~ the flux persisted ~~through~~ years of different environmental conditions. Soil moisture, WTL and air over time, and despite the high small-scale spatial variability, the temporal patterns of the fluxes were relatively similar across the chambers. Soil moisture as well as air and soil surface temperature were the most important variables explaining the temporal variation of N₂O fluxes. N₂O fluxes responded to precipitation events with peak fluxes measured on average 4 days after peaks in ~~in~~ the random forest, with lagged soil moisture and water table level. ~~The~~ also considered important. N₂O flux responded to soil wetting with a time lag of 1–7 days, but the length of the time ~~lags~~ lag varied in ~~space~~ spatially and between seasons indicating ~~possible~~ interactions with ~~temperature and~~ other ~~soil~~ spatially and temporally variable environmental conditions.

The high temporal variation in N₂O flux was related to a) ~~temporal variation in~~ seasonally variable environmental conditions, with the highest N₂O fluxes measured after summer ~~precipitation events~~ dry-wet cycles and

Formatted

Formatted: Highlight

Formatted: Highlight

Formatted: Highlight

Formatted: Highlight

Formatted: Highlight

Formatted: Highlight

Formatted: Highlight

Formatted: Highlight

Formatted: English (United States), Highlight

Formatted: English (United States), Highlight

Commented [HR1]: The sentence was updated to better match with the modified results section

winter soil freezing, and b) to annually ~~varying~~ variable seasonal weather conditions, ~~with the highest~~ N₂O emissions measured during wet summers and winters with discontinuous snow cover. Climate change may thus increase winter N₂O emissions, which may be offset by lower summer N₂O emissions in dry years. The high sensitivity of N₂O fluxes lead to seasonal high year to year variability in N₂O budget. Changes especially in the frequency of summer precipitation events and in winter temperature and snow conditions may increase the variability of annual N₂O emissions if the variability in summer and winter weather conditions suggests increasing variability in annual peatland forest N₂O budgets as the frequency of extreme weather events, such as droughts, is predicted to increase. ~~increases due to climate change.~~

Commented [RH2]: Link to future climatic conditions was made stronger

Formatted: Highlight

Formatted: Highlight

Formatted: Highlight

1. Introduction

Among the greenhouse gases, whose emissions contribute to climate change, nitrous oxide (N₂O) is one of the most potent, ~~is nitrous oxide (N₂O)~~, with a 100-year global warming potential ~~273~~ 260 times greater ~~stronger~~ than that of carbon dioxide (ForsterMyhre et al., 2021), 2013). A major part of N₂O ~~the emissions of N₂O~~ originates from soils (Butterbach-Bahl et al., 2013; Davidson and Kanter, 2014). ~~Human, and human~~ impact through altered nitrogen (N) cycling ~~eyele~~, land use and climate change affect the soil N₂O emissions in both ~~in~~ natural and managed ecosystems (Tian et al., 2018, 2020). The urgent need to mitigate climate change has evoked a broad interest in better understanding and estimating N₂O emissions of different ecosystems (Thompson et al., 2019; Shakoor et al., 2021). However, the accurate estimation of N₂O emissions has remained a challenge and emissions estimates continue to have relatively high uncertainties (Tian et al., ~~2020~~ 2018), 2020). A large part of the uncertainty in N₂O emission estimates ~~is due to~~ ~~comes from~~ inadequate understanding of the temporal and small-scale spatial variability of N₂O fluxes (Sutton et al., 2007; Groffman et al., 2009; Kuzyakov and Blagodatskaya, 2015; Wang et al., 2020).

Commented [HR3]: Time scale was added and GWP updated according to most recent IPCC report

Formatted: Highlight

Commented [HR4]: The sentence was split into two.

N₂O is formed in multiple processes, each favored by different soil conditions (Butterbach-Bahl et al., 2013). The main processes producing N₂O in soils are nitrification and denitrification (Bollmann and Conrad, 1998; Zhu et al., 2013; Hu et al., 2015). Nitrifying bacteria turn ammonium into nitrate in aerobic conditions. Nitrate produced in nitrification can further be reduced to nitric oxide, N₂O and gaseous nitrogen (N₂) in oxygen-limited or anaerobic conditions (Wrage et al., 2001; Zhu et al., 2013; Wrage-Mönnig et al., 2018), making ~~the availability of oxygen~~ ~~content~~ a key control of N₂O flux (Song et al., 2019). Oxygen limitation in soil and substrate availability for microbes is affected by soil water content, which makes N₂O production also sensitive to varying soil moisture conditions (Butterbach-Bahl et al., 2013). Along with soil moisture, substrate availability is widely affected by human actions, such as fertilization, nitrogen deposition and drainage of organic soils, which are all linked to increased N₂O fluxes (Pärn et al., 2018; Tian et al., 2020; Lin et al., 2022). Soil temperature regulates microbial activity in the soil, but it also shapes microbial community composition and affects N₂O production through, for example, frost, ice formation and thaw (Holtan-Hartwig et al., 2002; Risk et al., 2013; Wagner-Riddle et al., 2017).

Temporal variation of soil conditions ~~and substrate availability~~ can lead to a high temporal variation of N₂O flux within a year (Groffman et al., 2009; Kuzyakov and Blagodatskaya, 2015). Soil freeze-thaw and dry-wet cycles are examples of changes in soil conditions shown to shape seasonal variation in N₂O emissions (Risk et al., 2013; Congreves et al., 2018). High temporal variation ~~of N₂O flux~~ has been shown to be typical for ~~N₂O flux in~~ several

75 ecosystems (Luo et al., 2012; Molodovskaya et al., 2012; Anthony and Silver et al., 2021), but understanding related
76 to the temporal variation of N₂O production is limited by sparse sampling intervals of manual flux measurements, lack
77 of short-interval measurements and poor temporal coverage of data from all parts of the year (Barton et al., 2015;
78 Grace et al., 2020). Since short periods of high N₂O fluxes can account for a substantial amount of the annual N₂O
79 budget (Molodovskaya et al., 2012; Ju and Zhang, 2017; Anthony and Silver, 2021), capturing N₂O flux peaks and
80 understanding the causes of temporal variation of N₂O flux are essential for estimating annual emissions accurately.

81 ~~High~~ Similar to temporal variation, high spatial variation is ~~also typical~~ ~~common~~ for N₂O flux (~~Groffman et~~
82 ~~al., 2009). Estimating N₂O emissions accurately requires integrating information about the temporal and spatial~~
83 ~~dynamics. Variation in N₂O flux~~ occurs on multiple spatial scales, from large-scale variation between ecosystems to
84 small-scale variation within a few meters (~~Groffman et al., 2009; Ojanen et al., 2010; Krichels and Yang, 2019~~). High
85 N₂O fluxes are typically measured in ecosystems with high N availability, such as in agricultural fields and in drained
86 organic soils where fertilization and organic matter mineralization provide N supply for N₂O production (Maljanen et
87 al., 2003; Reay et al., 2012; Leppelt et al., 2014; Pärn et al., 2018). Within an ecosystem, varying soil properties and
88 conditions such as organic matter content, soil moisture or pH can create spatial variability in the N₂O fluxes
89 (Jungkunst et al., 2012; Giltrap et al., 2014). Although the small-scale spatial variation of N₂O flux can be large and
90 exceed the spatial variation between more distant parts of the same ecosystem (Yanai et al., 2003; Jungkunst et al.,
91 2012; Giltrap et al., 2014), the causes of small-scale spatial variability of N₂O ~~flux~~ are poorly known and little studied,
92 especially with short-interval measurements. Several questions related, for example, to the persistence of spatial
93 patterns over time and linkages between the spatial and temporal variation of N₂O flux are little understood.

94 Drained peatland forests are examples of ecosystems with relatively high N₂O fluxes and high spatio-
95 temporal variation of those fluxes (Maljanen et al., 2003; ~~Minkkinen et al., 2020; Ojanen et al., 2010; Pärn et al., 2018~~).
96 In Finland, about 60 % of the original peatland area has been drained for forestry (Korhonen et al., 2021), ~~which~~. The
97 ~~drainage~~ has resulted in a lowered groundwater level and increased N availability ~~for N₂O production~~ from the
98 decomposing peat. ~~Drainage has led~~, leading to increased N₂O fluxes, especially in nutrient-rich peatland forests with
99 a low C:N ratio (Martikainen et al., 1993; Laine et al., 1996; Klemetsson et al., 2005). The focus of previous studies
100 on peatland forest N₂O fluxes has been ~~mainly~~ on understanding the large-scale spatial variation of N₂O fluxes
101 between ~~different~~ peatland forests (Klemetsson et al., 2005; Ojanen et al., 2010; Minkkinen et al., 2020) and reporting
102 N₂O ~~flux fluxes for the studied peatland forest sites in~~ response to ~~forest~~ harvesting ~~or other forestry operations~~
103 (~~Maljanen et al., 2003; Huttunen et al., 2003; Korkiakoski et al., 2019, 2020~~). ~~Temporal~~ The temporal variation ~~has~~
104 ~~been mainly studied with sparse~~ of N₂O flux as well as its linkages to smaller-scale spatial variation of the flux are not
105 well understood, and only one snapshot of short-interval ~~chamber~~ N₂O measurements (~~Maljanen et al., 2010; is~~
106 ~~available from drained boreal peatland forest~~ (Pihlatie et al., 2010).

107 For the first time in boreal ~~drained peat soils~~ peatlands and non-agricultural boreal ecosystems, we use
108 ~~multiple~~ several years (2015–2019) of automated chamber ~~N₂O fluxes~~ ~~to measure~~ N₂O flux to gain a more
109 ~~comprehensive understanding of the spatio-temporal dynamics of N₂O flux~~. We investigate the characteristics of
110 temporal and small-scale spatial variation in N₂O flux. ~~We~~ and link the temporal variation of N₂O flux to seasonally
111 and annually variable environmental conditions including immediate and time-lagged responses. This is done to

Formatted: Default Paragraph Font, Font: (Default)
+Body (Calibri), 11 pt

Formatted: English (United States)

112 provide a more comprehensive understanding of the spatio-temporal dynamics of N₂O flux and to
 113 reduce uncertainties in current and future N₂O emission estimates in boreal peatland forests and beyond.

115 **2. Materials and methods**

116 **2.1. Site description**

117 The flux measurements were conducted between the 1st of June, made in 2015 and 29th of September, 2019
 118 in Lettosuo, a drained nutrient-rich peatland forest located in southern Finland (Lettosuo, 60°38' N, 23°57' E). The
 119 mean annual mean temperature in the area is 5.2 °C, and the mean annual precipitation is 621 mm according to the
 120 long-term weather record from the nearest automatic weather station (Jokioinen Ilmala, 1991–2020, 35 km from the
 121 study site). The site was initially first drained in the 1930s and more intensively in 1969 to promote enhance tree
 122 growth. Ditches were dug about 1 m deep and 45 m apart. The site was fertilized with phosphorus and potassium after
 123 the later drainage. The relatively low C:N ratio reflects the fen history of the site (Table 1). Ditches were dug in 1969
 124 about 1 m deep with 45 m spacing. Drainage lowered the groundwater table level, resulting in a transition to boreal-
 125 forest-like vegetation. The ground vegetation consisted mainly of dwarf shrubs (*Vaccinium myrtillus*, *Vaccinium vitis-*
 126 *idaea*) and herbaceous plants (*Lysimachia europaea*, *Dryopteris carthusiana*) with sedges (*Carex globularis*,
 127 *Eriophorum vaginatum*) and Sphagnum mosses (*Sphagnum russowii*, *Sphagnum girgensohnii*) in patches. The
 128 relatively low C:N ratio reflects the fen history of the site (Table 1).

129 Before March 2016, the site was a mixed forest with an overstory dominated by Scots pine (*Pinus sylvestris*)
 130 and an overstory, while the understorey dominated by consisted of mostly Norway spruce (*Picea abies*). Both
 131 overstorey over and understorey contained included a small amount number of downy Downy birch (*Betula pubescens*).
 132 Overstorey pines were removed during a selection harvest in March 2016, overstorey pine trees were harvested (70
 133 % of the total stem volume; Korhikoski et al., 2020, 2023). The, but the surroundings of the measurement
 134 chamber chamber used in this study were harvested more lightly, and the chamber area. The study plots continued to
 135 have a high coverage of spruce and birch. The selection harvest after the overstorey pine trees were removed in the
 136 harvesting. The partial harvesting did not affect N₂O fluxes according to the previous study from the site (Korhikoski
 137 et al., 2020), and the effect of the harvest harvesting was left out of the focus of this study.

138 **Table 1: Soil properties at the study site. Values represent general soil properties at the study site before**
 139 **the selection harvest forest harvesting was done. Data from Korhikoski et al. (2019).**

Depth	Total-N (%)	Total-C (%)	C:N	Bulk density (g cm ⁻³)
Humus	1.7 ± 0.4	56.2 ± 2.3	33.2 ± 2.3	0.01 ± 0.003
0–10 cm	2.2 ± 0.2	55.2 ± 2.1	24.9 ± 2.1	0.12 ± 0.03
10–20 cm	2.5 ± 0.2	58.9 ± 1.6	23.8 ± 1.6	0.18 ± 0.02

Commented [RH5]: More detailed information about the automatic chamber system, environmental variable measurements, turbulence-problem and analysis was added to the material and methods section (+400 words)

Commented [HR6]: Exact dates were added

Formatted: Highlight

Formatted: Highlight

Commented [HR7]: Distance to the nearest weather station was added.

Commented [HR8]: The term partial harvest was changed to selection harvest which is more official term for the harvesting type.

Formatted: Font: 9 pt, Not Bold

Formatted: Caption

Formatted: Font: 10 pt

Formatted: Font: 10 pt

146 2.2. Automatic chamber flux measurements

147 The N₂O flux between the forest floor and the atmosphere was measured using with six
148 automated automatically operating chambers. The transparent, acrylic, rectangular cuboid chambers with the
149 dimensions 57 x 57 x 40 cm (length x width x height) were placed to sample the spatial variation of the ground
150 vegetation composition and were located within an area of 15 x 20 m (Fig. 1). Distance to the closest ditch and trees
151 also varied between chambers (Table S1). The chambers were placed on permanently installed steel collars that were
152 inserted into the soil to about 2 cm depth of 2 cm. All the chambers closed automatically for six minutes once an
153 hour year-round. The chambers resulting in 6 x 24 flux measurements per day. Chambers had an air temperature
154 sensors measuring the headspace temperature and a fan to mix the air inside the chamber headspace. During
155 winters, chambers were cleaned from snow and ice every 1–3 weeks and snow depth inside the chambers was
156 measured to account for the effect of snow depth on chamber volume. During the winter 2016–2017, extension collars
157 were used to better allow snow to fit inside the chambers.

158 The N₂O concentration of the chamber headspace air was measured using a continuous wave quantum
159 cascade laser absorption spectrometer (LGR-CW-QCL N₂O/CO-23d, Los Gatos Research Inc., Mountain View, CA,
160 USA) that was placed in the measurement cabin close to the chambers (Fig. 1b). The analyzer had an accuracy of
161 0.01 ppb per second, corresponding to a minimum detectable flux (Nickerson, 2016) of 0.06 μg N₂O m⁻² h⁻¹ in our
162 chamber system. During each chamber closure, air from the closed chambers sample air, was pumped into the analyzer
163 and back to the chamber headspace through plastic tubes (length 15 m, flow about 1 l/min). After each. The same
164 chamber closure, the airflow measurement system, was switched to the next chamber. Ambient air was measured for
165 at least 1 min between the chamber closures to allow concentrations in the tubes to stabilize back to the ambient level.
166 Concentration data from the first 30 s of each chamber closure were not used in flux calculation to avoid possible
167 pressure disturbance caused by the closing chamber affecting the flux (Pavelka et al., 2018). For more information
168 about the automatic chamber system, see the previous also in other studies from covering N₂O, CO₂ and CH₄ fluxes of
169 the same site (Koskinen et al., 2014; Korkiakoski et al., 2017, 2020). Measurements in Chamber 6 ended six months
170 earlier (April 2019) than measurements in other chambers due to problems in chamber functioning.

171 N₂O fluxes were calculated similarly to Korkiakoski et al. (2017), but by using a linear fit. The mean
172 headspace temperature of the to the N₂O concentration change during the chamber closure and air pressure measured
173 at the site were used in the flux calculation. Calculated fluxes were filtered using normalized root mean square error
174 threshold and an iterative standard deviation filter to remove erroneous fluxes resulting from chamber malfunction.
175 A more detailed description of the flux calculation and filtering can be found in Korkiakoski et al., 2017). Daily mean
176 N₂O fluxes from each chamber (2020). The fact that the fans were used in the analysis because the automatic chamber
177 system seemed not adjusted according to create an artificial the wind conditions likely created some diurnal cycle of
178 N₂O from which the possible natural diurnal cycle could not be separated. The artificial diurnal cycle was caused by
179 the difference in turbulence between the ambient air and chamber headspace in the flux, as discussed previously
180 reported for CO₂ and CH₄ fluxes at the same site (Koskinen et al., 2014; Korkiakoski et al., 2017). During calm
181 periods, especially during summer nights, the transfer of N₂O from soil pores to the atmosphere slowed down, leading
182 to increased N₂O concentration in the soil. When the chamber closed and the turbulence increased because of the fan,

Commented [HR9]: Information about the chamber maintenance in winter was added.

Formatted: Indent: First line: 1,27 cm

Formatted: Highlight

Formatted: Highlight

Formatted: Highlight

Formatted: Highlight

Formatted: Highlight

Commented [RH(10)]: We added more detailed information about the automatic chamber measurement system and analyzer, including minimum detectable flux in the system, flow rate and information about the ambient measurements.

Formatted: Highlight

Commented [RH(11)]: Mention about the use of measured air temperature and air pressure in the flux calculation was added.

Formatted: Highlight

Formatted: Highlight

Commented [RH(12)]: More detailed explanation about the artificial diurnal cycle was added.

Formatted: Highlight

Formatted: Highlight

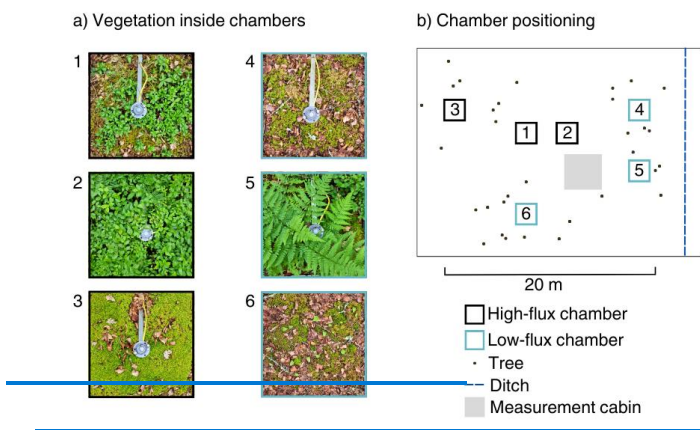
Formatted: Highlight

Formatted: Highlight

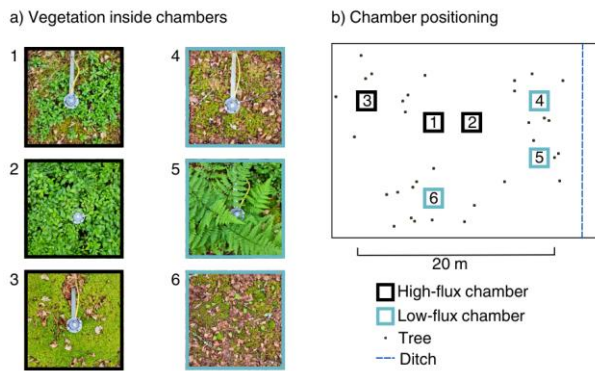
183 the N₂O from the soil pores was vented to the chamber headspace air, leading to overestimated flux. The opposite
 184 phenomenon probably occurred in windy conditions, resulting in underestimated flux. Based on our experience,
 185 automatic chamber fluxes measured in drained peatlands with dry and porous peat soil are particularly sensitive to
 186 2017). To minimize the possible effect of artificial diurnal variation in N₂O flux, daily mean fluxes were used in this
 187 phenomenon (Koskinen et al., 2014; Korhonen et al., 2017). Hourly N₂O flux peaks were not typical in the flux
 188 data, and daily mean N₂O fluxes thus well represent the main characteristics of the temporal variation. It should be
 189 noted that the artificial diurnal cycle creates an additional source of uncertainty in the reported N₂O budgets study.

Formatted: Highlight

Formatted: Highlight



191



192

193 **Figure 1:** (a) Vegetation inside the six chambers and (b) the positioning of the chambers on the forest floor
 194 in relation to the nearest ditch and trees. Chambers are named from one to six based on the maximum
 195 measured flux with Chamber 1 having the highest measured flux. Chambers 1–3 with black edges are
 196 classified as “high-flux chambers” and Chambers 4–6 with blue edges as “low-flux chambers”. For more
 197 information on chamber vegetation, ditches and trees, see Table S1. (Sect. 3.2).
 198

Commented [HR13]: Measurement cabin was added in the figure

Formatted: Highlight

199 **2.3. Environmental variables**

200 Several environmental variables were measured to link the temporal variation of N₂O fluxes with the
201 environmental conditions. Air temperature was measured at 2 m height below the forest canopy (HMP45D, Vaisala
202 Oyj, Vantaa, Finland). Soil surface temperature was measured at 2 cm depth in each chamber and the soil temperature
203 at 5 cm depth at one location close to the chambers (Pt100, Nokeval Oy, Nokia, Finland). Soil moisture was measured
204 at one location about 75 m from the chamber measurement location at 7 and 20 cm depths (Delta-T ML3, Delta-T
205 Devices Ltd, Cambridge, UK). The soil moisture data were used to describe the temporal variation of soil moisture,
206 assuming that the soil moisture had relatively similar temporal patterns across the study site. The rather than the
207 absolute level of soil moisture in each at the chamber may have differed from location. We assumed that the measured
208 soil moisture, and the possibility of differences in the temporal variation of soil moisture between the logger and
209 conditions represent the conditions near the chambers cannot be excluded. Soil moisture data relatively well since the
210 microtopography, surface vegetation and shading by the canopy, were used together with water table level and
211 precipitation data to strengthen the conclusions related to soil water conditions. The measurements of air and soil
212 temperatures were ongoing throughout the study period, but the soil moisture measurements ended half a year earlier
213 than automatic chamber measurements (April 2019). relatively similar in both locations.

214 Water table level (WTL) below the soil surface was measured hourly using automatic loggersprobes
215 (TruTrack WT-HR, Intech Instruments Ltd, Auckland, New Zealand; Odyssey Capacitance Water Level Logger,
216 Dataflow Systems Ltd, Christchurch, New Zealand) placed into dipwells that were installed into the ground.
217 Chambers 1–2 and 3–4–5 shared a WTL loggersensor that was placed in-between the chamber pairs. two chambers,
218 and Chambers 3 and 6 had their own WTL loggersensors next to the chambers, chamber collar. Since WTL
219 measurements for Chambers 3, 4, 5 and 6 started half a year later than chamber measurements (in December 2015),
220 WTL during this and other data gapsbefore that was modeled for each chamber using randomRandom forest with
221 conditional inference trees (Hothorn et al., 2006). WTL data from Chambers 1–2, seven other WTL loggers at the
222 study site and Other WTL measurements near the automatic chambers, precipitation and soil moisture were used as
223 explanatory variables in the gap-filling model. Modeling was done first for the logger with the least amount of missing
224 data, after which the gap-filled WTL time series was added to the model as an explanatory variable to increase the
225 predictive power of the model for the variables with more missing data models (evaluation data R² = 0.90–0.97).

226 Precipitation was measured at the site throughout the study period (Casella Tipping Bucket Rain Gauge,
227 Casella Solutions Ltd, Bedford, UK; OTT Pluvio2 L 400 RH, OTT Hydromet Ltd, Kempten, Germany) and daily
228 cumulative precipitation sum was calculated, used. The precipitation data measured atin the nearest weather station
229 was used to gap-fill winters and other measurement gaps in precipitation data measured at the site (correlation of
230 precipitation between sites 0.65, p < 0.05). Snow depth was measured atin the nearest weather station wasand used to
231 describe general snow conditions experienced each winter.

232 Thermal seasons were used to analyze the seasonality of N₂O fluxes. The thermal seasons were defined
233 according to typical Finnish standards (Ruosteenoja et al., 20162014; Finnish Meteorological Institute, 2023), and by
234 using air temperature data fromof the site (Appendix A). During thermal winter, daily mean air temperature was
235 persistently below 0 °C, during summer above 10 °C and during thermal spring and autumn between 0 and 10 °C.

Commented [RH(14): Explanation about the weaknesses of soil moisture measurements was made more clear.

Formatted: Highlight

Formatted: Highlight

Formatted: Highlight

Formatted: Highlight

Formatted: Highlight

Commented [HR15]: Explanation about the measurement period times for environmental variables added

Commented [HR16]: Typo in chamber number was corrected

Formatted: Highlight

Commented [HR17]: Explanation about the explanatory variables used in modelling WTL was clarified

Formatted: Highlight

Formatted: Highlight

Formatted: Highlight

Commented [HR18]: Measurement period times for environmental variables were added

236 Seasons based on months ~~were~~ used to compare conditions measured at the site with ~~seasonal~~-long-term averages
237 reported ~~monthly~~ for the nearest ~~automatic~~ weather station.

238
239

240 -2.4. Identifying high-flux periods

241 The term “high-flux period” was used to describe periods of elevated flux, including periods from moderately
242 increased flux to the highest flux peaks. ~~“High”~~The term ~~high-flux period”~~ was used instead of a commonly used “hot
243 moment” ~~term~~ because the definition of a hot moment largely varies between studies, with sometimes only extremely
244 high fluxes being considered as hot moments (Molodovskaya, 2012; Krichels ~~and Yang, et al.,~~ 2019; Anthony and
245 Silver, 2021; Song et al., 2022).

246 ~~To identify the high-flux periods, their length, seasonality, and starting conditions, to numerically describe~~
247 ~~the temporal patterns of N₂O fluxes, different thresholds to separate high-flux days from the baseline days were tested.~~
248 ~~Finally, a common percentile threshold of 70 % was used in all chambers. High fluxes were measured less frequently~~
249 ~~compared to the more common low fluxes, which made high-flux days distinct from the more common baseline days~~
250 ~~in flux histograms of all chambers (Fig. S2). Any percentile threshold between 60–80 % separated high-flux days~~
251 ~~from the more common baseline fluxes relatively well, and the mean of these (70 %) was used. The mean N₂O flux~~
252 ~~of the study period was close to the chosen 70 % percentile threshold in all chambers. Days with the mean flux above~~
253 ~~the 70 % percentile were classified as high-flux days and the rest of the days as baseline days. -~~

254 The length of each high-flux period was the number of days the flux remained above the 70 % percentile,
255 including possible data gaps within this period. The high-flux period was set to continue over ~~a~~the data gap if three
256 days before and after the data gap were classified as high-flux days. A three-day marginal was chosen to ensure that
257 short one-to-two-day peaks would not create long-lasting high-flux periods over ~~the~~data gaps. If the high-flux period
258 started from a data gap or ended to it, the start or end date of the high-flux period was set to the first or last measured
259 day, respectively. ~~Pearson correlation was used to test how similar the temporal patterns of N₂O flux were between~~
260 ~~chambers.~~

261 ~~Pearson correlation was used to test correlation between N₂O flux time series of different chambers and~~
262 ~~multiple linear regression was used to test if each environmental variable could explain differences in the flux patterns~~
263 ~~between chambers. In the multiple linear regression, N₂O flux of each chamber was explained by flux of one other~~
264 ~~chamber, and ability of each environmental variable to explain the remaining variance was tested one environmental~~
265 ~~variable at the time.~~

266
267

267 2.5. Machine learning

268 Machine learning models were used to improve understanding of the temporal controls on N₂O flux,
269 including a possible effect of time lags between environmental conditions and N₂O ~~flux.~~ ~~Since the models were run~~
270 ~~separately for the six chambers, the models also allowed estimation of whether the temporal variation is controlled~~
271 ~~similarly in the different chambers.~~ The machine learning approach was used because machine learning models do
272 not rely on mathematical functions to describe relationships between variables and are able to account for interactions

Commented [RH(19)]: The purpose of high-flux period identification is now shortly described and explanation about high-flux period identification was clarified.

Formatted: Highlight

Formatted: Highlight

Formatted: Highlight

Formatted: Highlight

Formatted: Highlight

Formatted: Highlight

Formatted: Highlight

Formatted: Highlight

Formatted: Highlight

Formatted: First Paragraph

273 between variables [flexibly \(Olden et al., 2008\)](#), ~~without having to include them in the equation by hand (Olden et al.,~~
274 ~~2008). This is particularly useful when using a large dataset with multiple environmental variables to model N₂O~~
275 ~~fluxes whose controls and mathematical forms of responses are not yet fully understood.~~

276 The Random forest algorithm, developed by Breiman (2001), is a classification tree-based method that uses
277 bootstrap aggregation of a model training data and a randomly chosen subset of explanatory variables ([mtry-parameter](#))
278 to train each classification tree. In bootstrap aggregation, a subset of data is taken from the model training data with
279 or without returning it to the original training data. The part of data that is not bootstrapped to train trees is called out-
280 of-bag (OOB). OOB data ~~and it~~ can be used to evaluate model performance, ~~since this part of the data is not used~~
281 ~~during the model training phase.~~ In each ~~random~~Random forest tree, the bootstrapped data are classified into
282 subgroups and further ~~into~~ smaller subgroups by setting threshold values for the randomly chosen subset of
283 explanatory variables. The setting of the threshold values is done to maximize the information gain until no further
284 thresholds, also called splits, can be made. After a selected number of trees are built, the final model prediction can
285 be made using the average of all the trees (continuous response) or the most common outcome (categorical response).

286 Random forest variable importance (VI) metrics show the importance of each explanatory variable in
287 explaining variation in the response variable. ~~VI~~Variable importance metrics can be biased if the ~~data type and scale~~
288 ~~of the~~explanatory variables ~~correlate~~vary or if there is a correlation between explanatory variables (Strobl et al., 2007).
289 Therefore, we used ~~random~~Random forest with conditional inference trees (Hothorn [et al., 2006](#)) that allowed us to
290 get more accurate ~~VI~~variable importance measures in the presence of correlated explanatory variables and their time-
291 lagged versions. Compared to trees in ~~random~~Random forest, conditional inference trees use a p-value-based splitting
292 criterion to classify the bootstrap aggregated data in the building phase of each tree. As suggested by Strobl et al.
293 (2007), in the presence of correlated explanatory variables, variable importance metrics from the conditional inference
294 trees were calculated using conditional permutation importance.

295 Chamber-specific models had [daily mean](#) N₂O flux as the response variable and the measured temperature
296 variables (air, [soil 2 cm and 5 cm depths](#)), soil moisture (7 and 20 cm [depths](#)), WTL and daily cumulative precipitation
297 as explanatory variables. ~~Periods~~Time lags of ~~missing data in environmental variables were gap-filled using the~~
298 ~~random forest proximity tool RFimpute (Liaw and Wiener, 2002).~~ ~~One-to-seven days' time-lagged versions of each~~
299 ~~environmental variable~~7 days were added as ~~additional~~explanatory variables ~~to for all the models besides unlagged~~
300 ~~environmental~~explanatory variables. The imbalanced ~~distributions~~distribution of N₂O fluxes ~~as model predictors~~ were
301 corrected with the SMOGN algorithm (Abd Elrahman and Abraham, 2013). The subset of data to train each tree was
302 bootstrapped without replacement with a sample size 0.632 times the size of the training dataset, as suggested by
303 Strobl (2007). Models were trained with 500 trees and ~~random~~Random forest default *mtry* for continuous response
304 variable was used (*mtry* = number of explanatory variables / 3).

305 The first three years of data were utilized as the model training period (~~1~~June 2015 ~~—~~1 June 2018), and this
306 data were further split into 70 % training data and 30 % evaluation data to test model performance within the training
307 period. The fourth year of measurements until soil moisture measurements ended (~~1~~June 2018 ~~—~~4 April 2019) was
308 left aside for evaluation to test model performance outside the training period. The ~~performance~~prediction accuracy
309 of the models ~~on different~~in each evaluation ~~datasets~~data was analyzed using R squared (R²) and root mean squared

Formatted: Highlight

Formatted: Highlight

Commented [HR20]: Short description about gapfilling environmental variables was added

310 error (RMSE). R^2 was used to compare model performance between chambers. Variable selection was not done.
311 Evaluation results are presented in appendices (Appendix B).
312 VIs and accumulated local effects (ALE) were used to interpret the modeling results. For easier comparison
313 of VIs across chambers, the VIs of each chamber Variable importance values were scaled from between zero to and
314 one (0 = least important variable, 1 = most important variable) and the total VIs of each variable were calculated (total
315 $VI = VI$ of unlagged variable + VIs of lags) to enable comparison between chambers. The ALE Accumulated local
316 effects (ALE) method by Apley and Zhu (2020) was used to visualize the response of N_2O flux to environmental
317 conditions and their lags in the models. In ALE figures, ALE value (y-axis) zero refers to the mean predicted N_2O
318 flux, with a positive ALE value meaning larger and a negative value lower predicted N_2O flux in a specific
319 environmental condition (x-axis). ALE values for lagged environmental variables indicate the response of predicted
320 N_2O flux to previous environmental conditions. From the unlagged and lagged versions of each environmental
321 variable, the one that received the highest ALE value for a given environmental condition was considered to represent
322 the typical response time of N_2O flux to that condition. In this article, the response time, or lag length in the presence
323 of at least a one-day lag, refers to the time it takes for N_2O to reach peak flux after the onset of a given environmental
324 condition. The reported evaluation results (RMSE, R^2), VIs, and ALE values are averages over 10 model runs.

325

326 2.6. Gap-filling and N_2O budgets

327 Data gaps covered 12–24 % of the study period depending on the chamber. Daily mean Most gaps occurred
328 at the same time in all chambers. Notable is that measurements in Chamber 6 ended six months earlier in 2019 than
329 measurements in other chambers. N_2O flux time series were gap-filled to calculate N_2O budgets. Gap-In other analysis,
330 gap-filled data were not used in other analyses to avoid additional uncertainty of the results arising from the gap-
331 filling.

332 Gap-filling was done by training the Random forest with conditional inference trees on the whole
333 measurement period (4.5 years) data with 30 % data excluded for evaluation. The same models and explanatory
334 variables were used in the models as in the machine learning part analysis, including time-lagged variables. The fourth
335 measurement year previously left for evaluation was also included in the training data for gap-filling. To test the
336 performance of the gap-filling model, separate models were run with 70 % and 30 % split to the training data and
337 evaluation data, respectively. Evaluation metrics (RMSE, R^2) results of gap-filling models are shown in Appendices
338 (Appendix B). Gap-filled daily mean N_2O fluxes were used to calculate cumulative N_2O budgets flux for each chamber
339 in each thermal season and year. The uncertainty uncertainties related to the N_2O budgets was were assumed to be a
340 combination of uncertainty related to flux measurement and uncertainty related to gap-filling. Detailed information
341 about the calculation of the uncertainty can be found in Korhikoski et al. (2017).

342 Flux calculation was performed in the Python programming language version 2.7 (Van Rossum and Drake,
343 1995). Data preparation and analysis were performed in R statistical software version 4.0.5 (R core team, 2021).
344 Cforest-command in the party package (Hothorn et al., 2006; Strobl et al., 2007; Zeileis et al., 2008) was used to
345 perform random for Random forest with conditional inference trees. Data and simplified R-code about the machine
346 learning part of the study are made freely available (See Sect. 7).

Commented [RH21]: The use of evaluation metrics was clarified.

Formatted: Highlight

Commented [HR22]: Explanation about how VIs are interpreted was clarified.

Formatted: Highlight

Formatted: Highlight

Formatted: Highlight

Commented [HR23]: Explanation of ALE and its interpretation in the presence of lags were made more clear

Formatted: Indent: First line: 1,27 cm

Commented [HR24]: R code for the modeling part was also made available.

347
348
349
350
351
352
353
354
355
356
357
358
359
360
361
362
363
364
365
366
367
368
369
370
371
372
373
374
375
376
377
378
379

3. Results

3.1. Environmental conditions

The seasonal temperature conditions were variable for the years 2015–2019 (Fig. 2). The summers (June, July, August) 2015 (14.1 °C) and 2017 (14.4 °C) were colder (seasonal means 14.1 °C and 14.4 °C, respectively) than the long-term average (15.6 °C, Jokioinen-Ilmala 1991–2020), and, while winters (December, January, February) 2015–2016 (–3.4 °C), 2016–2017 (–3 °C) and 2018–2019 (–3.5 °C) were warmer (seasonal means –3.4 °C, –3.0 °C and –3.5 °C, respectively) than the long-term average (–4.3 °C) (Fig. Jokioinen-Ilmala, 1991–2020; 2). Temperatures were warm in all seasons in during the years 2018 and 2019 were warmer than the long-term average, with the summer (seasonal mean 17.2 °C) and autumn (seasonal mean 6.7 °C) 2018 being particularly especially warm compared to the long-term averages (summer average temperatures 15.6 °C and autumn 5.4 °C, respectively).

The area received the least amount of precipitation in 2018 (annual sum 434 mm) and the most precipitation in 2017 (annual sum 657 mm) with, when the long-term annual average being was 621 mm. The Winter 2015–2016 (67 mm) was wet, while autumn 2016 (36 mm), winter 2016–2017 (24 mm) and summer 2018 (seasonal sum 44 mm) was especially were dry compared to the long-term average summer precipitation of 71 mm. The drought that began in the spring 2018 continued until averages (winter 44 mm, autumn 58 mm and summer 71 mm).

Soil conditions measured at the site varied between seasons and years (Fig. 3). Soil moisture was at 7 cm was on average lower in winters (0.26 m³ m⁻³) and springs (0.22 m³ m⁻³) compared to summers (0.31 m³ m⁻³) and autumns (0.33 m³ m⁻³). Soil moistures at 7 cm and 20 cm were continuously lower than the mean means of the study measurement period (0.28 and 0.56 m³ m⁻³, respectively) from the summer 2018 until the end of the study measurement period (Fig. 3), with WTL was deeper than the mean of the study period mean being 0.28 m³ m⁻³ for 7 cm soil moisture and 0.56 m³ m⁻³ for 20 cm soil moisture. WTL was on average (–36 cm and continuously deeper than that) in the summer and autumn 2015 as well as in the summers 2018 and 2019. Soil surface temperatures varied on average between –0.6 °C in winter and 14.0 °C in summer with small differences in soil surface temperatures between chambers. Soil temperatures at 5 cm depth reached freezing below zero temperatures in winters 2015–2016 (min. –3.8 °C), 2016–2017 (min. –1.8 °C) and 2017–2018 (min. –0.33 °C). Variation of –0.33 °C with most days with negative soil 5 cm temperatures in winters 2015–2016 and 2016–2017. Temporal variation in air and soil surface temperatures was high greater in winters 2015–2016 and 2016–2017. The compared to the latter two years of the measurement period. All winters had a period or periods of snow cover was thickest with the maximum measured snow depth being the greatest, in winter 2018–2019 (max. 52 cm) and thinnest the lowest, in winter 2016–2017 (max. 11 cm). The number of days with snow cover was lower in winters Winters 2015–2016 (85 days) and 2016–2017 (93 days), and higher in had days with snow cover less than winters 2017–2018 (125 days) and 2018–2019 (116 days).

Commented [RH(25)]: Results section was shortened (-450 words). Things that are not discussed in the discussion were removed. Sentences were made more compact and easier to read by removing chamber- and year-specific details that are not important.

Formatted: Highlight

Commented [RH(26)]: Values inside parentheses are explained better. Words mean, min., max. or sum were added or parentheses moved next to the in-text explanation. Some sentences are re-formatted.

Formatted: Highlight

Formatted: Highlight

Formatted: Highlight

Formatted: Highlight

Formatted: Highlight

Formatted: Highlight

Formatted: Highlight

Formatted: Highlight

Formatted: Highlight

Formatted: Highlight

Formatted: Highlight

Formatted: Highlight

Formatted: Highlight

Formatted: Highlight

Formatted: Highlight

Formatted: Highlight

Formatted: Highlight

Formatted: Highlight

Commented [HR(27)]: Some of the values inside parentheses were moved to the actual text.

Formatted: Highlight

Formatted: Highlight

Formatted: Highlight

Formatted: Highlight

Formatted: Highlight

Formatted: Highlight

Formatted: Highlight

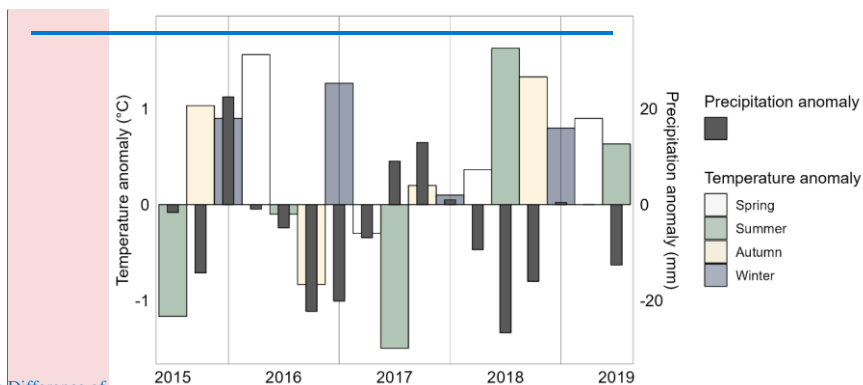
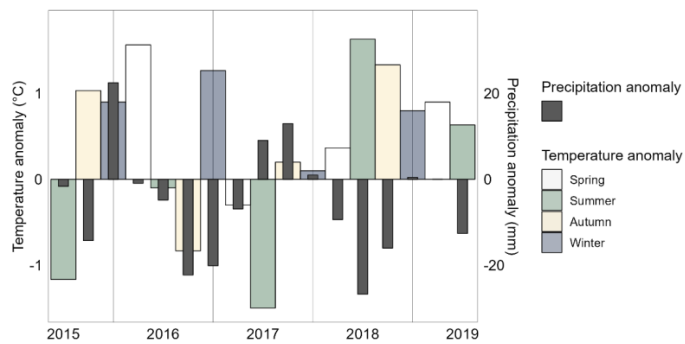


Figure 2: Difference of

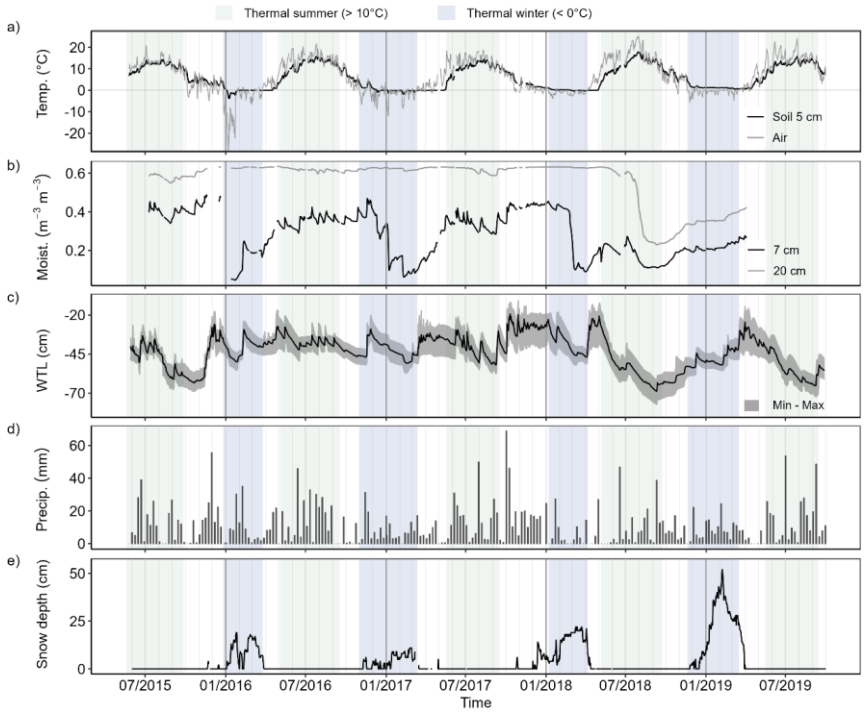
Figure 2: Seasonal temperature and precipitation anomalies during the measurement period. The seasonal mean air temperature and seasonal cumulative precipitation sum from the long-term average. The of each year is compared to the long-term seasonal averages fromat the nearest weather station are used (Jokioinen Ilmala, 1991–2020). Seasons are based on months (autumn: September–November, winter: December–February, spring: March–May and summer: June–August).

Formatted: Highlight

Formatted: Highlight

Commented [RH(28)]: Figure caption was made more clear

Formatted: Highlight



389
390
391

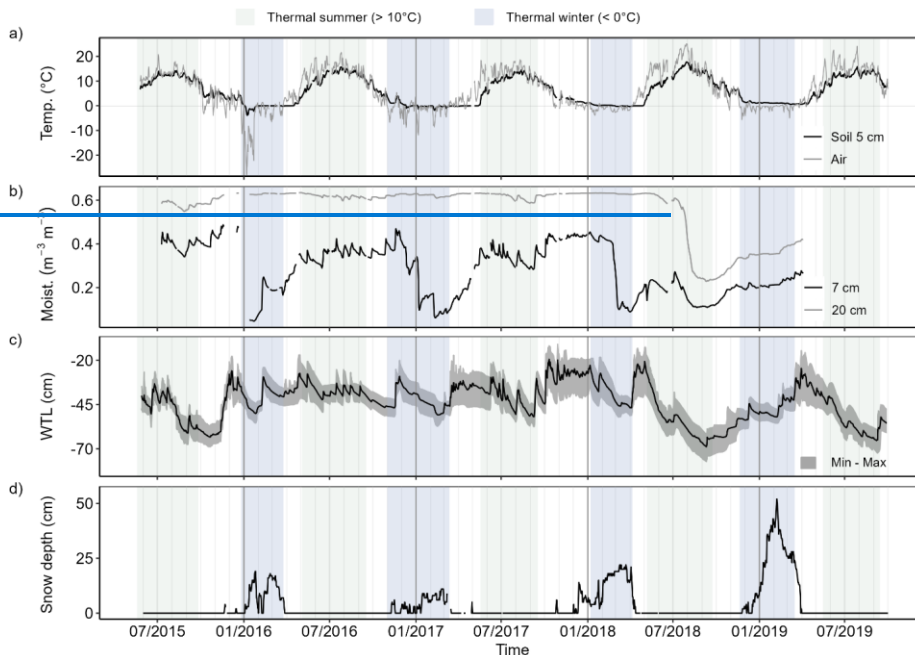


Figure 3: (a) Daily mean air and soil temperatures (5 cm depth), (b) soil moisture (7 and 20 cm depths), (c) water table level (WTL), (d) weekly precipitation sum and (e) daily mean snow depth. WTL is the mean of the chambers with gray shading showing values measured next to the range of WTL between different chambers, with variation between the lowest and highest WTL indicated with shading. Snow depth was measured at the nearest weather station. Data are not gap-filled. For the definition of thermal winter and summer, see Sect. 2.3.

Commented [HR29]: Precipitation was added to the figure

Formatted: Highlight

3.2. Temporal and spatial variation of N₂O flux

The daily mean N₂O flux varied between -10 and +1760 μg N₂O m⁻² h⁻¹ during the 4.5 years of measurements (Fig. 4), and chamber mean N₂O flux between +20 (Chamber 6) and +140 μg N₂O m⁻² h⁻¹ (Chamber 1) (Table 2). The annual mean flux was the highest in 2016 or 2017, depending on the chamber, and smallest in 2018 in all chambers (Table S3.1). Mean fluxes in 2015 (June–December) were lower than in the whole years of 2016 and 2017 but higher than in 2018. Mean fluxes in 2019 (January–September) were generally higher than the mean fluxes in the whole year 2018.

Three chambers (Chambers 1, 2 and 3) had maximum daily mean fluxes greater than 1100 μg N₂O m⁻² h⁻¹, and while the other three chambers (Chambers 4, 5 and 6) had maximum daily mean fluxes less than 400 μg N₂O m⁻² h⁻¹ (Table 2). Chambers 1–3 also. The mean and the range of the daily mean N₂O fluxes varied between years and chambers, but the high flux chambers generally had a high range and mean flux higher than Chambers 4–6 (the low flux chambers) in all years (Table S3.1). The annual differences in the mean flux was the highest and the range of the mean daily flux between high flux and low flux chambers were the largest in 2016 and 2017, depending on the chamber, and lowest (the smallest) in 2018 and 2019. Based on the differences especially in the maximum flux,

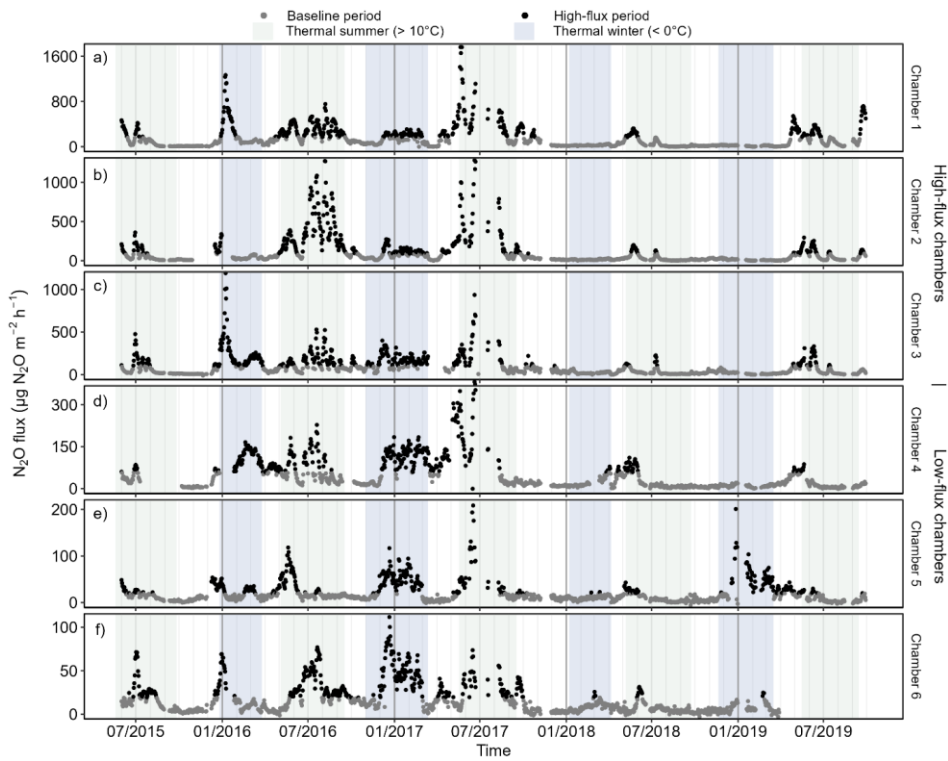
414 ~~standard deviation fluxes~~ and ~~in~~ the range of the flux variation, Chambers 1–3 were classified as “high-flux chambers”
415 and Chambers 4–6 as “low-flux chambers”.

416 ~~The chamber~~ Chamber-specific 70 % percentiles that were used to define ~~the~~ high-flux periods from the
417 baseline periods (~~Seet. 2.4~~) ranged from 20 (~~Chamber 5 and 6~~) to 170 $\mu\text{g N}_2\text{O m}^{-2} \text{h}^{-1}$ (~~Chamber 1~~, Table 2). The
418 length of the individual baseline periods varied ~~from between~~ 1 ~~to and~~ 330 days with a mean of 26 days, while the
419 length of the high-flux periods varied between 1 and 134 days with ~~thea~~ mean of 11 days.

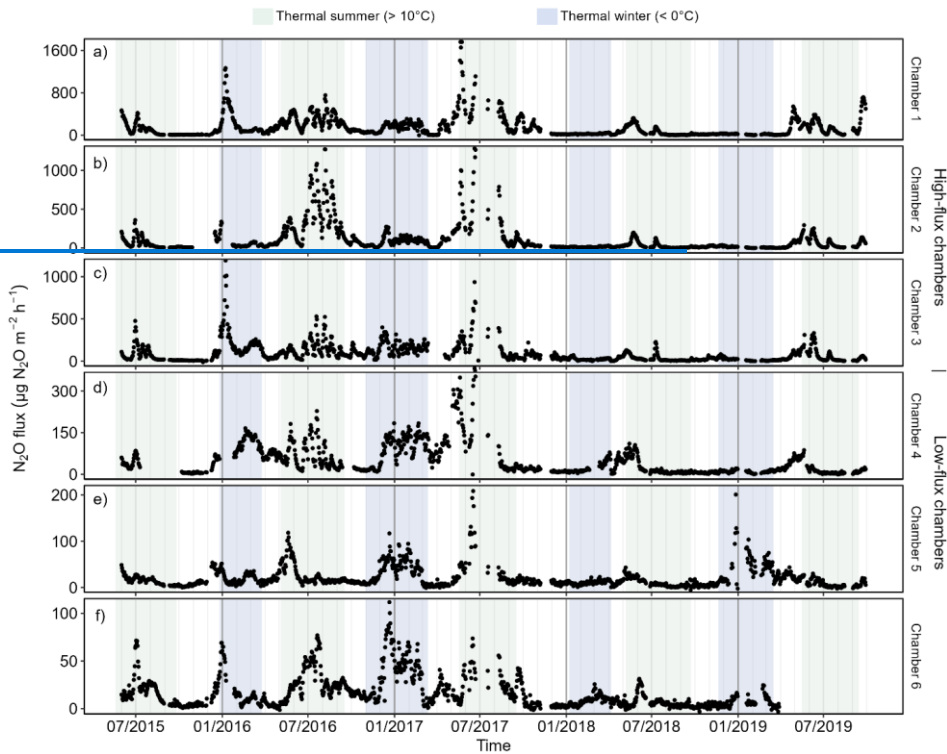
420 The ~~correlatione~~relations of the flux time series ~~betweenfor each pair of~~ chambers ~~were positive and~~ varied
421 between 0.79 (Chambers 1 and 2) and 0.29 (Chambers 1 and 4) (Table S4). ~~Correlation was 1~~. ~~Correlations were~~ the
422 highest between the chambers with a similar range of N_2O flux: among high-flux chambers, ~~correlatione~~relations
423 varied between 0.64–0.79 and among low-flux chambers, between 0.46–0.49. ~~Differences~~Soil surface and soil 5 cm
424 ~~temperatures explained the differences~~ in ~~WTL~~ N_2O fluxes between ~~chambers were~~most chamber pairs statistically
425 ~~significant but were not associated with the spatial variation of N_2O flux.~~ significantly (Fig. S4.2).

426

Formatted: First Paragraph



427



428
 429 **Figure 4:** Daily mean N₂O flux measured in the six automatic chambers in 2015–2019. Fluxes from different
 430 chambers are shown in panels (a–f) ordered by maximum daily mean N₂O flux. Chambers are grouped into
 431 **high-flux** (Chambers Chamber 1, 2 and 3) and **low-flux** chambers (Chambers Chamber 4, 5 and 6). The
 432 scale of the y-axis is chamber specific and fluxes are not gap-filled. **Periods Thermal winter** refers to a period
 433 with the daily mean fluxes > 70 % percentile are classified as high-flux periods air temperature persistently
 434 < 0 °C and thermal summer to a period with daily mean air temperature persistently > 10 °C.
 435

Commented [HR30]: High-flux and baseline days are now coloured differently

Formatted: Highlight

Formatted: Font: Not Italic

436 **Table 2:** Minimum, maximum, mean, median, 70 % percentile and standard deviation (SD) of daily mean
 437 N₂O fluxes over the study period. The unit is 4.5 years for each chamber. Unit of the flux is µg N₂O m⁻² h⁻¹.
 438 Percentile thresholds (70 %) were used to define high-flux periods. Year-specific statistics can be found in
 439 [Table S3.1](#).
 440

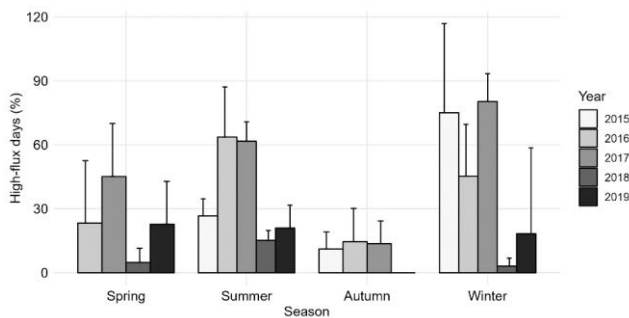
Source	Min	Max	Mean	Median	Percentile 70 %	SD
Chamber 1	-1	1761	143	73	168	193
Chamber 2	-1	1282	99	34	88	171
Chamber 3	-12	1192	87	46	100	112
Chamber 4	-1	381	48	22	58	57
Chamber 5	-5	244	20	13	20	23
Chamber 6	-3	112	17	11	19	17

441

442 3.3. Seasonality of N₂O flux

443 The highest N₂O daily fluxes were measured during the thermal summers (Chambers 1, 2, 4 and 5) or winters
 444 (Chambers 3 and 6) depending on the chamber. The fluxes mean seasonal N₂O fluxes calculated for thermal seasons
 445 were also on average the highest in for the thermal summers and/or winters, and the lowest in autumns (Tables S3).
 446 throughout the study period. The mean N₂O flux was the smallest in autumn in all years and chambers. The percentage
 447 of measurement days identified as high-flux days averaged was on average 24 % in spring, 38 % in summer and 44
 448 % in winter and, while the thermal autumns had 9 % in autumn days identified as high-flux days (Fig. 5). The highest
 449 proportion of high-flux days in each season varied between years with the highest proportions of winter and high-flux
 450 days measured in 2015 and 2017, and the highest proportions of summer high-flux days were measured in summers
 451 2016 and 2017, and the lowest proportion in 2018. Variation in the percentage of high-flux days between chambers
 452 was greatest for thermal winters.

453



454

455 **Figure 5: Mean occurrence of high-flux days out of measured days in different thermal seasons and standard**
 456 **deviation between chambers.**

457

458 In spring, N₂O fluxes increased steadily as started to increase when soil surface temperature temperature
 459 increased above zero (Fig. 6 and S5), with most of the spring high-flux periods starting at soil surface temperatures
 460 0–2 °C (Fig. 7). Spring N₂O fluxes steadily increased steadily with increasing soil temperatures, and flux peaks
 461 were peak top was reached in late spring or early summer. Summer increased summer N₂O fluxes were measured after
 462 peaks in soil moisture and WTL, the highest N₂O fluxes being reached typically several days after soil moisture and
 463 WTL peak. Most summer high-flux periods started after precipitation events when soil moisture at moist soil
 464 conditions (7-cm was 0.37–0.41 m³ m⁻³) and during relatively high WTL (between 35 to and 50 cm depth) (Fig.
 465 7), but the peak fluxes were reached several days after the rain events. The Autumn high flux period starting
 466 conditions for soil moisture and WTL in were similar to the summer, but increased N₂O fluxes were reached a longer
 467 period of time after soil moisture and WTL peak. Soil temperatures at the autumn start of the high-flux periods were

Formatted: Highlight

Formatted: Highlight

Formatted: Highlight

Formatted: Highlight

Formatted: Highlight

Formatted: Highlight

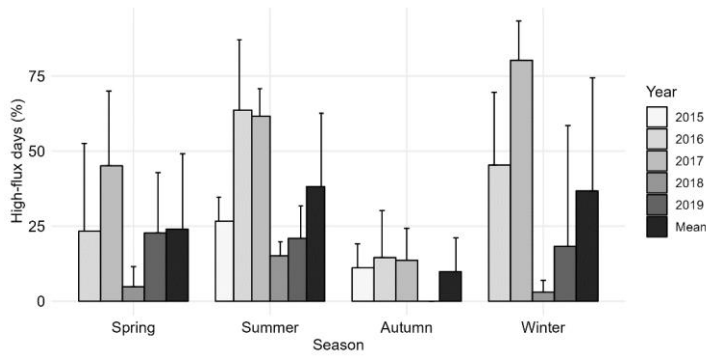
Formatted: Highlight

Commented [HR31]: Results shown in plot 7 are discussed more also in the text

468 similar to those in summer, but the response to soil wetting was slower and fluxes were smaller, lower in autumn
 469 compared to summer.

470 Winter high-flux periods started on soil temperatures close to 0 °C (Fig. 7). In early winter, the N₂O fluxes
 471 increased when soil temperatures at the soil surface and 5 cm depth decreased close to near zero and
 472 below that, with further increase in flux measured if soil temperature also at 5 cm depth decreased below zero (Fig. 6
 473 and S5). Later in 6, 7, S5). After the initial freezing peak, early winter N₂O flux started to decrease after the soil
 474 temperatures increased close to or above zero. Later during the winter, increased N₂O fluxes were measured during
 475 periods of soil freezing or when soil temperatures increased towards close to or above zero after soil freezing. Freezing
 476 of the soil surface did not typically lead to high N₂O fluxes without temperatures being below zero also at 5 cm depth.
 477 The response to soil freezing, especially in the early winter, was stronger than the response to soil thawing in terms of
 478 duration of the high-flux periods and peak flux. An exception to that was Chamber 5 during winter 2018–2019, where
 479 high N₂O fluxes were measured during the mid-winter despite freezing temperature measured only at the surface soil.
 480 Temporal variation of N₂O fluxes within winter were also related to the temporal variation in soil surface and air
 481 temperature, with N₂O fluxes varying more in winters 2015–2016 and 2016–2017 with higher temporal variation in
 482 temperature compared to other winters.

483



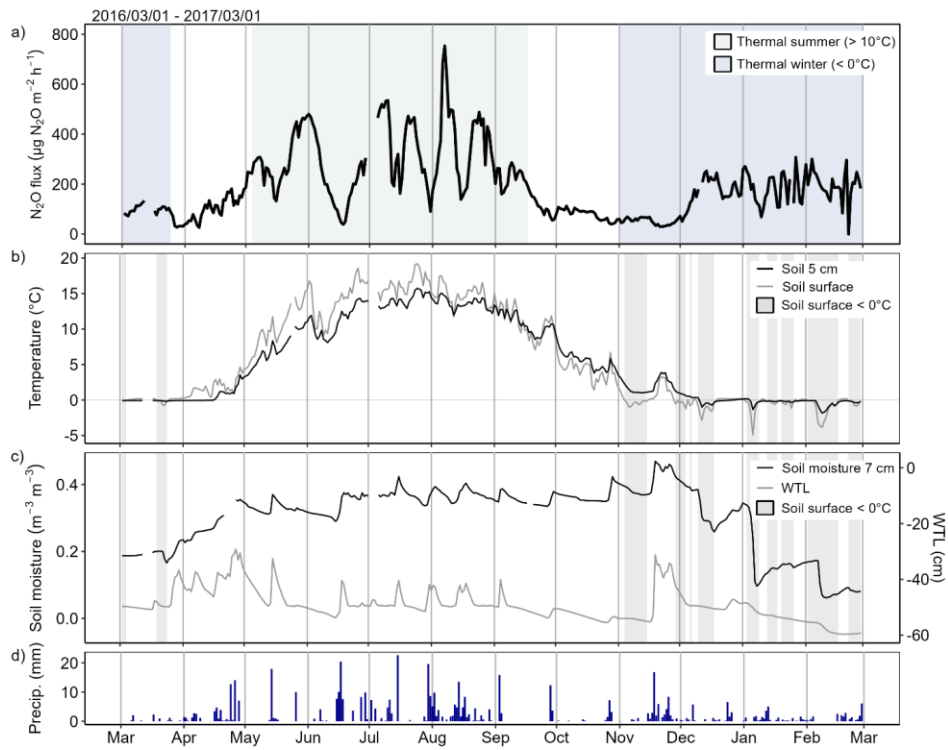
484

485 **Figure 5: Occurrence of high-flux days out of measured days in different thermal seasons. Bars show annual**
 486 **means across different chambers and error bars show standard deviation between chambers. Mean bars show**
 487 **the mean across the years. The bar for winter 2019 only contains winter days between January – March 2019.**
 488

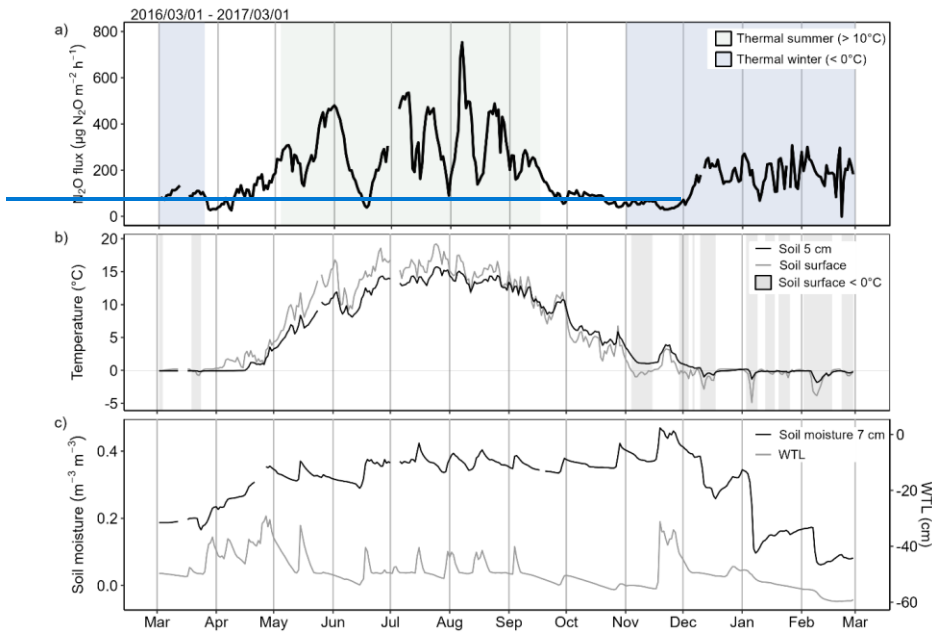
Commented [HR32]: Mention about the stronger response to early winter freezing was added since it's discussed later.

Commented [HR33]: Figure was updated: The bar for winter 2015 was removed because it contained only few days (no measurements at the beginning of 2015 and winter started late in December). Means across years were also added.

Commented [HR34]: Figure caption was made more clear



489

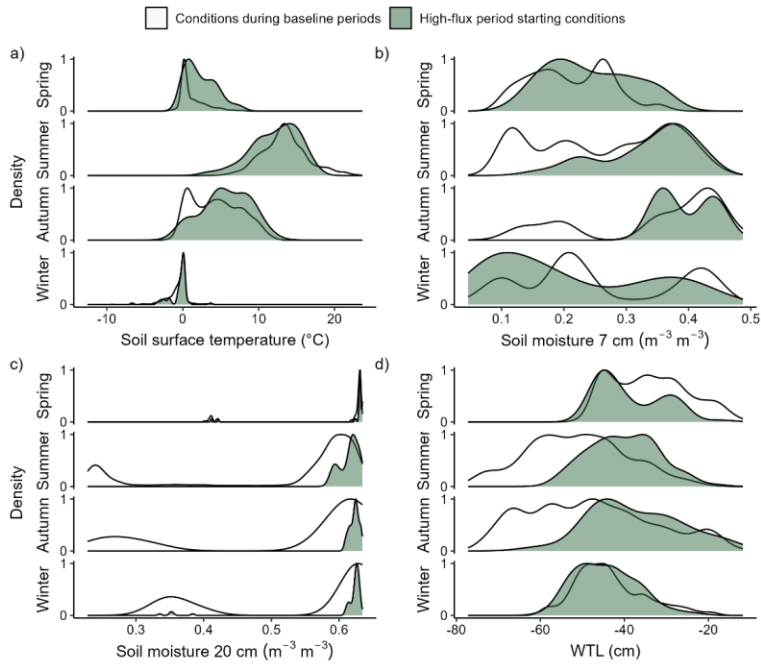


490
 491 **Figure 6:** (a) Daily mean N₂O flux, (b) soil surface temperature and temperature at 5 cm depth with
 492 highlighted freezing periods (soil surface temperature < 0 °C), (and c) soil moisture and water table level
 493 (WTL), and (d) daily precipitation from MarchFebruary 2016 to March 2017 in Chamber 1. The temporal
 494 variation of N₂O flux in Chamber 1 was similar to the other chambers, but the range of flux variation was
 495 larger compared to the low-flux chambers. The shown temporal dynamics of N₂O flux were measured in a
 496 year with relatively wet summer and warm winter. Data are not gap-filled. Figures for other chambers are
 497 presented in the supplements (S5).
 498

Commented [HR35]: Precipitation was added to the figure and shading for soil surface temperature <0°C was added also to panel c.

Formatted: Highlight

Formatted: English (United States)



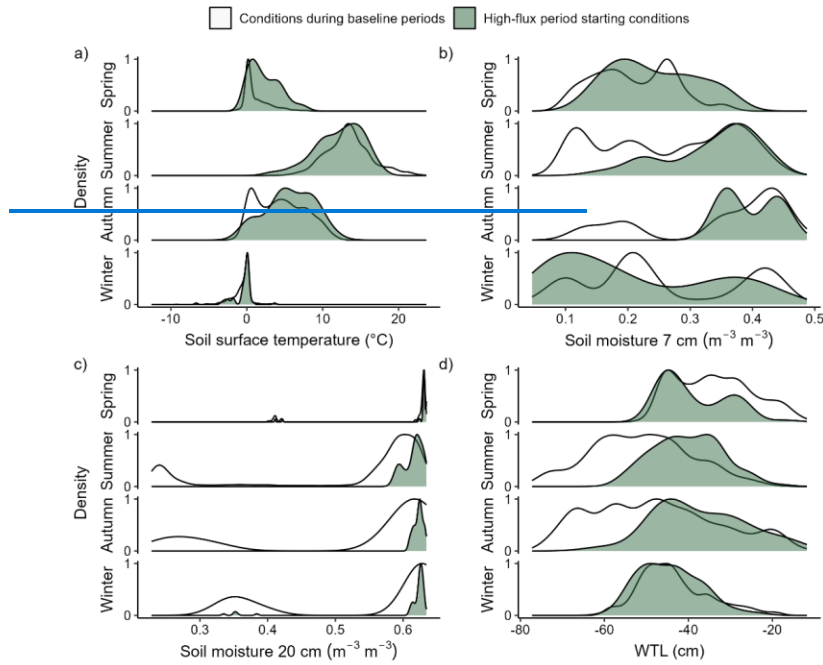


Figure 7: High-flux period starting conditions in each season compared to conditions outside the high-flux periods. Density plots show the distribution of high-flux periods starting on different (a) soil surface temperatures, (b) soil moistures at 7 cm depth, (c) soil moistures at 20 cm depth, (d) and water table levels (WTL). The Y-axis shows scaled (0–1) proportion (%) of high-flux periods starting on conditions shown on the x-axis (1=most common high-flux periods starting condition, 0=no starting high-flux periods). Panels in each plot show density distribution for each thermal season. For comparison, the variation in soil conditions during baseline periods is also shown (1=most common baseline period condition, 0=no such condition measured during baseline periods). All years and high-flux periods of all chambers are included. Density distribution values on y-axis are scaled (0–1).

Commented [HR36]: Figure caption was made more clear to help readers to interpret the figure

Formatted: Highlight

Formatted: Highlight

Formatted: Highlight

Formatted: Highlight

Formatted: Highlight

Formatted: Highlight

Formatted: Highlight

Formatted: Highlight

Formatted: Highlight

Formatted: Highlight

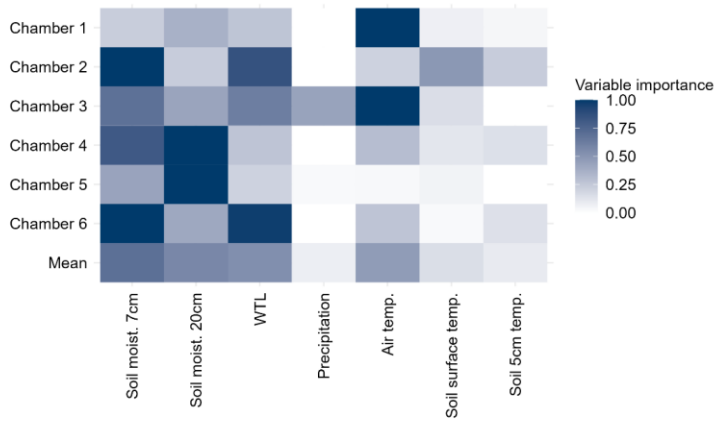
Formatted: Highlight

Formatted: Highlight

Commented [RH(37)]: The amount of details in the text was decreased and the text updated to match the new VI figure

3.4. Machine learning modelling results

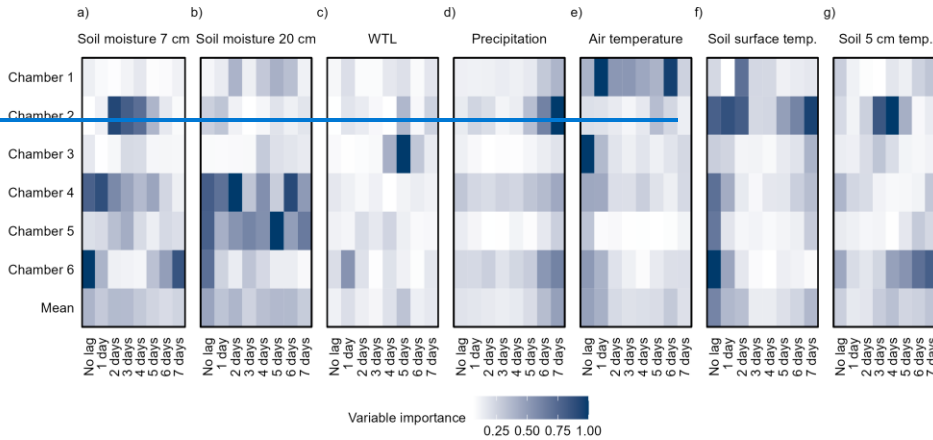
Soil moisture (both 7 and 20 cm), air temperature and WTL were considered to be the most important variables explaining the temporal variation of N₂O flux (Fig. 8) with the mean total variable importance (VI, 0 = no importance, 1 = high importance) being 0.7 and 0.6 for soil moisture (7 and 20 cm respectively) and 0.5 for air temperature and WTL. The mean VI of lags (1–7 days) for each environmental variable was the highest for 7 and 20 cm soil moisture (mean VI 0.3 for both) with 5 cm soil temperature and air temperature also having importance on lags (mean VI 0.25 and 0.20, respectively, Fig. S6). Lags of other variables received mean VIs lower than 0.1, but precipitation had an increasing VI towards the longest lags (6–7 days).



519
 520 **Figure 8: Total variable importance (VI)** Unlagged soil moistures at 7 cm and 20 cm had mean variable importance
 521 (VI) scores 0.43 and 0.45 (respectively, 0 = lowest importance, 1 = highest importance) when VI scores were averaged
 522 across chambers (Fig. 8). Lagged (1–7 days) soil moisture variables received on average VI score of 0.31 (7 cm soil
 523 moisture) and 0.33 (20 cm soil moisture). The average VI score for unlagged air temperature was 0.45 and for soil
 524 surface temperature 0.24 and the variable importance generally decreased with increasing lag time. Unlagged soil
 525 temperature at 5 cm received VI score of an average 0.27 and increased VI scores also for lagged variables with the
 526 mean across lags 0.25. VI scores for WTL were on average 0.04 with little importance for lagged WTL in most
 527 chambers. Precipitation received VI score of 0.06 and increasing importance with increasing lag time. The most
 528 important variable and the importance of their individual lags varied between chambers with either soil moisture,
 529 WTL or air temperature receiving the highest VI score. High flux chambers received high VI scores also for lagged
 530 temperature variables that were less important in low flux chambers.

Commented [HR38]: Figure changed and caption updated. The new figure shows total VIs of variables instead of lag-specific and unlagged VIs. This was done to strengthen the conclusions and avoid mis-understandings made from the detailed plot.

Lag-specific VIs are presented in the supplements.



532 **Figure 8: Variable importance (VI) scores of different environmental variables in explaining the temporal**
 533 **variation of N₂O flux in random forest with conditional inference trees. Total VI is the sum of VIs of unlagged**
 534 **and lagged (1–7 days) and their lagged versions of the variable. Rows in the in explaining the temporal**
 535 **variation of N₂O. The matrix plot show VIs shows VI values separately for different chambers and (Chambers**
 536 **1–6) as well as the mean VIs VI across all the chambers (Mean). VI values are means across 10 runs of Random**
 537 **forest with conditional inference trees. VI scores are scaled between 0 and 1 (0 = no lowest importance, 1 =**
 538 **highest importance) per chamber. Lag-specific VIs are shown in Fig. S6 to make VI scores comparable across**
 539 **chambers.**
 540
 541

542 Accumulated local effects (ALE) curves for unlagged 7 cm soil moisture showed that the highest N₂O fluxes
 543 generally predicted on soil moisture values close to 0.3 m³·m⁻³ or below 0.1 m³·m⁻³ (Fig. 9 and S6). On moist
 544 conditions (> 0.3 m³·m⁻³), the highest fluxes were predicted for the 1–7 days lagged soil moisture when the soil was
 545 moist (> 0.35 m³·m⁻³). The lag- Predicted flux was typically the highest if soil moisture had been greater than 0.4 m³
 546 m⁻³ 3–7 days ago. On low 7 cm soil moistures (< 0.3 m³·m⁻³), the highest N₂O fluxes were predicted for unlagged soil
 547 moisture with the highest predicted flux varied from 1 to 7 days little differences between chambers with a mean lag
 548 of 4 days. Predicted fluxes were also high when 20 cm soil moisture (> 0.6 m³·m⁻³), predicted N₂O flux increased
 549 with increasing soil moisture in all chambers. Predicted flux on high 20 cm soil moisture was low (< 0.1 m³·m⁻³,
 550 frozen soil) the highest for lagged soil moisture only in two chambers. For WTL, the predicted flux was generally
 551 high the highest when WTL was high (> 45 cm), with the highest predicted flux on average for 4 days lagged WTL.
 552 The predicted flux for unlagged WTL was low at high WTL, while the predicted had been closer to the soil surface
 553 than 30 cm 3–7 days ago. The highest flux for unlagged WTL increased with decreasing WTL was typically predicted
 554 for WTL deeper than 50 cm. In all chambers, N₂O flux was predicted to be the highest for 4–7 days after lagged
 555 precipitation with an average lag of 5 days between chambers when daily precipitation had been at least if rainfall had
 556 been about 5 mm or more.

557 For On temperatures above 5°C, the predicted N₂O fluxes increased with increasing air and soil surface
 558 temperatures above 5 °C, the predicted fluxes increased with increasing temperature, with the highest predicted fluxes
 559 at air temperatures above taking place when air and soil temperature exceeded 15 °C and soil temperatures above 10

Formatted: Highlight

Formatted: Highlight

Formatted: Highlight

Formatted: Highlight

Formatted: Highlight

Formatted: Highlight

Formatted: Highlight

Formatted: Highlight

Formatted: Highlight

Commented [RH(39)]: Text was updated to make it more clear. The length of lags are also listed and lags-effects of WTL and precipitation are discussed more.

Formatted: Highlight

Formatted: Highlight

Formatted: Highlight

Formatted: Highlight

Formatted: Highlight

Formatted: Highlight

Formatted: Highlight

Formatted: Highlight

Formatted: Highlight

Formatted: Highlight

Formatted: Highlight

Formatted: Highlight

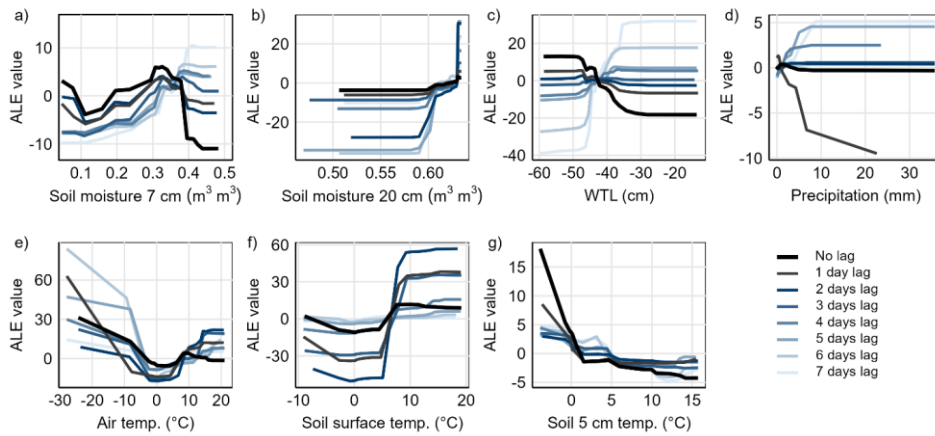
Formatted: Highlight

Formatted: Highlight

Formatted: Highlight

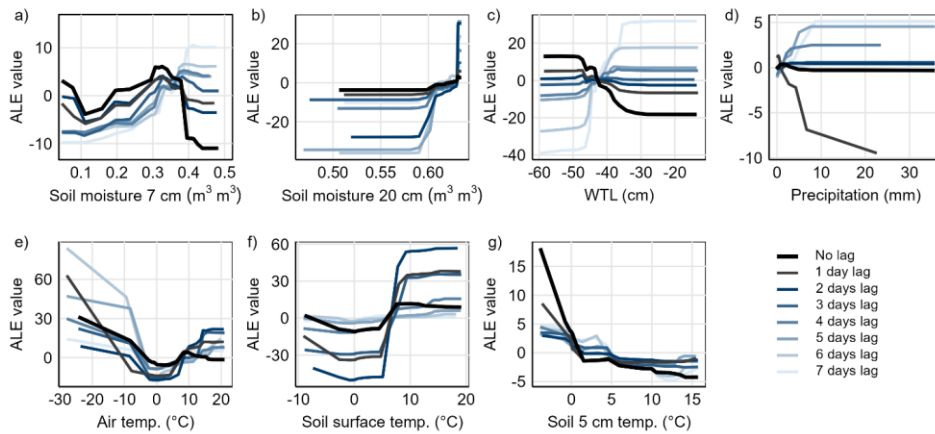
Formatted: Highlight

560 40 °C. For air and soil, respectively. Below about 0–2 °C temperatures (soil surface and 5 cm depth) below 0–2 °C,
 561 the predicted N₂O fluxes increased with decreasing air, soil surface and soil 5 cm temperature. In most chambers, the
 562 increase in the predicted flux for soil 5 cm temperature at 0–2 °C was particularly especially strong, with differences
 563 in the responses between immediate and lagged variables between chambers. Responses between lagged and unlagged
 564 temperature, soil surface and air temperature variables also varied among between chambers.



565

566



567

568 **Figure 9: Response of predicted N₂O flux to different environmental conditions for Chamber 1 visualized using Accumulated Local Effects (ALE). Figures illustrate how the predicted N₂O**
 569 **flux values deviate from the mean predicted flux (ALE = 0) along the gradients of (a) soil moisture at 7 cm**
 570 **depth, (b) soil moisture at 20 cm depth, (c) water table level (WTL), (d) precipitation, (e) air temperature, (f)**
 571 **soil surface temperature and (g) soil temperature at 5 cm. ALE responses for unlagged and lagged variables**
 572 **(1–7 days) are included. Lines represent the mean ALE values of 10 model runs. ALE responses for Chambers**
 573 **2–6 are presented in supplements (S7S6).**
 574

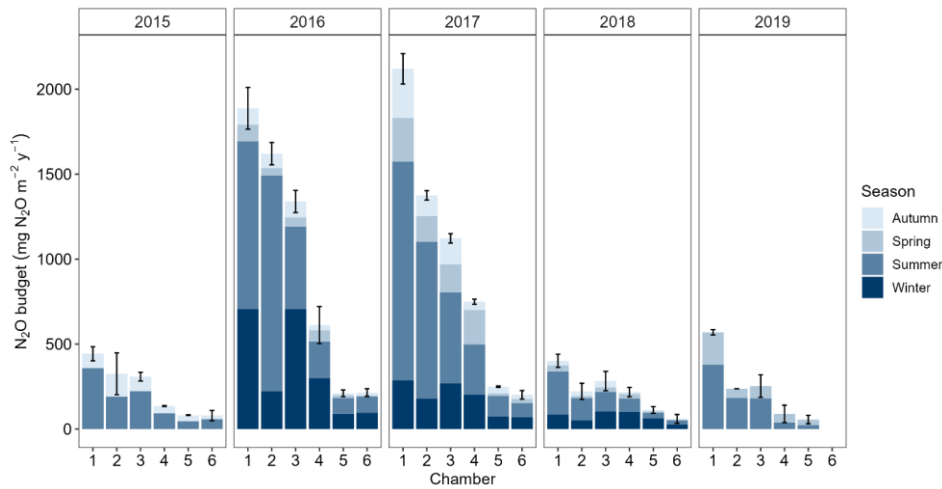
575

576 **3.5. N₂O budgets**

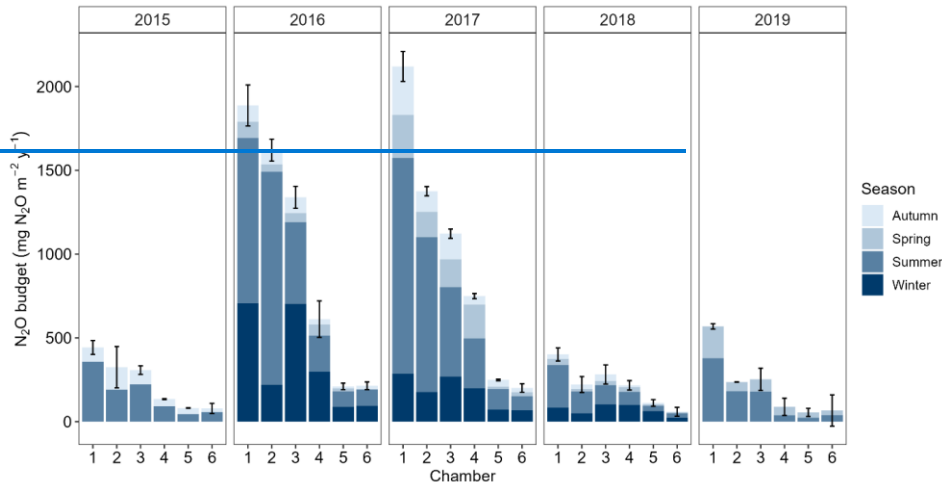
577 ~~The annual~~ Annual N₂O budgets of individual chambers varied between 60 (Chamber 6) and 2110 mg N₂O
 578 m⁻² y⁻¹ (Chamber 1) when considering the three full measurement years 2016, 2017 and 2018 (Fig. 10, Tables S8). In
 579 2016 and 2017, annual N₂O budgets were 1120–2110 mg N₂O m⁻² y⁻¹ in the high-flux
 580 chambers and 200–740 mg N₂O m⁻² y⁻¹ (Chambers 1–3) in the low-flux chambers. In 2018, the N₂O budgets were
 581 lower than 400 mg N₂O m⁻² y⁻¹ in all chambers in 2018. Winters and summers
 582 generally contributed generally the most to the annual N₂O budgets in all three years, with summers contributing on
 583 average 48 % and winters 34 % (Tables S8S7). The seasonal contributions of spring and autumn to the annual N₂O
 584 budgets were; on average 10 % per season, 9 % for spring and autumn. Summer N₂O budgets in partially measured
 585 years 2015 and 2019 were smaller than in 2016 and 2017 but, especially in high flux chambers, greater than in 2018.

586

- Commented [RH(40)]: Annual budgets written in a more clear way.
- Formatted: Highlight
- Formatted: Highlight
- Formatted: Highlight
- Formatted: Superscript, Highlight
- Formatted: Highlight
- Formatted: Highlight
- Formatted: Highlight



587



588 **Figure 10: Annual N₂O budgets for each chamber and measurement year with seasonal contributions. Only**
 589 **seasons that were completely within the measurement period (4.5 years) are included. The N₂O budget for**
 590 **the year 2015 only includes summer and autumn, and the N₂O budget for the year 2019 only spring and**
 591 **summer. Measurements in Chamber 6 ended in early 2019 and no budget is shown for that year. Thermal**
 592 **seasons are used. Error bars denote total uncertainty related to the total N₂O budget of the year.**
 593

Commented [RH(41): N2O budget of Chamber 6 in 2019 was removed because measurements ended already in early April (=no full seasons measured).

Formatted: Highlight

594
 595 **4. Discussion**

Commented [HR42]: Discussion was restructured to make it more compact. Main things are discussed and some of the less important things were left out (eg. Multiple regression results). (-400 words)

596 **4.1. Temporal variation of N₂O fluxes**

597 The measured peatland forest N₂O fluxes were relatively high compared to N₂O fluxes reported for from most
 598 of the other boreal and temperate forests on peat and/or mineral soils. The N₂O budgets of boreal peatland forests have
 599 mainly varied between -30 and 1200-920 mg N₂O m⁻² y⁻¹ (Alm et al., 1999; Arnold et al., 2005; Minkinen et al, 2020;
 600 Butlers et al., 2023), and in a similar range also in). The N₂O budgets of temperate mineral soil forests have varied
 601 within a similar range (Papen and Butterbach-Bahl, 1999; Luo et al., 2012). The N₂O budgets of our six automatic
 602 chambers are unlikely able to represent the N₂O budget of while the whole site, but the mean annual N₂O budget of
 603 the chamber area greater than 950 budgets in the present study were below 500 mg N₂O m⁻² y⁻¹ in 2018 in all
 604 measurement chambers, the annual N₂O budgets for three of the chambers exceeded 1000 mg N₂O m⁻² y⁻¹ in two full
 605 study years (2016 and 2017) out of three underlines the role of drained nutrient-rich peatland forest as hotspots for
 606 N₂O emission the three full measurement years, (Fig. 10). Similarly high or higher fluxes have been previously
 607 measured in peatland forest after clear-felling of the trees with especially logging residues linked with increased N₂O
 608 fluxes (Mäkiranta et al., 2012; Korkiakoski et al., 2019).

Formatted: Highlight

Formatted: Highlight

Formatted: Highlight

Formatted: Highlight

Formatted: Highlight

Formatted: Highlight

Formatted: Highlight

609 Nutrient-rich peat with a relatively low C:N ratio likely explains the high N₂O budgets of the chamber area.
 610 study site. Low C:N ratio may have also have increased the sensitivity of the N₂O fluxes to temporal variation in
 611 soil conditions (Klemetsson et al., 2005; Pihlatie Pihlatie et al., 2010); Hu et al., 2015). Although the selection harvest
 612 partial harvesting done at the site in the spring 2016 did not increase the N₂O budget of the harvested area compared

Commented [HR43]: More careful wording referring to the area the N2O budgets represent added.

Formatted: Highlight

Commented [RH(44): More careful wording referring to the area the N2O budgets represent were added.

613 to the control site according to Korhonen et al., (2020), the effect of ~~the harvest~~harvesting on N₂O fluxes of
614 individual chambers cannot be completely excluded. Since the N₂O budgets increased after harvesting in both ~~the~~
615 harvested site and in the control site (see Korhonen et al., 2020), most of the increase in N₂O budgets in the years
616 2016 and 2017 is likely explained by year-to-year variation in environmental conditions.

617

618 4.1. Seasonal variation of N₂O fluxes

619 Winters were characterized by N₂O flux peaks occurring during both freezing and thawing (Fig. 6, 7 and S5).
620 similar to those reported in earlier studies (Teepe et al., 2001; Maljanen et al., 2007; Maljanen et al., 2010). Freezing-
621 related N₂O emissions are likely explained by N₂O production in the remaining unfrozen water films that have
622 increased C and N content in the freezing soil (Maljanen et al., 2007; Congreves et al., 2018). Winter N₂O flux peaks
623 were measured when soil frost reached at least the 5 cm depth, whereas during winters with only shallow frost (< 5
624 cm, winters 2017–2018 and 2018–2019), high N₂O fluxes were less common. This indicates the importance of frost
625 depth for winter N₂O emissions. The importance of ground frost severity and depth has also been suggested by others
626 in several ecosystems (Nielsen et al., 2001; Koponen and Martikainen, 2004; Maljanen et al., 2007; Luo et al., 2012).
627 The importance of deeper soil freezing may indicate that the freezing-related N₂O fluxes mainly originate from the
628 freezing peat rather than from the surface litter layer, unlike suggested by Pihlatie et al. (2007) in a nutrient-poor
629 peatland forest. Low C:N ratio may have favored N₂O production in the ~~Considering~~ nutrient-rich peat (Klemetsson
630 et al., 2005). Site-specific differences in nutrient availability may influence the sensitivity of winter N₂O fluxes to
631 frost depth.

632 Winters with deeper soil frost and higher N₂O emissions (winters 2015–2016 and 2016–2017) were
633 characterized by discontinuous and shallow snow cover and variable temperature conditions (Fig. 3 and 4). Shallow
634 snow cover combined with alternating cold and warm weather in the first two winters of the study period have likely
635 increased the number of freeze-thaw cycles and their intensity leading to higher total N₂O fluxes (Maljanen et al.,
636 2007; Ruan and Robertson, 2017). The results suggest the possibility for increasing winter N₂O emissions from
637 drained peat soils if winters continue to warm, the occurrence of extreme temperature fluctuations increases and snow
638 cover in the southern boreal region becomes shallower.

639 Similar to freezing, soil thawing triggered N₂O emissions during winter freeze-thaw cycles, but emissions
640 ceased within a few days of the onset of the thawing phase even if soil temperature continued to rise (Fig. 6 and S5).
641 Similar short-term N₂O peaks in response to soil thawing have been measured also in laboratory experiments by Teepe
642 et al. (2001), and Koponen and Martikainen (2004). Thaw-related emissions have often been explained by increased
643 N availability in the thawing soil (Groffman et al., 2006; Wagner-Riddle et al., 2017), and the cause of the short pulse
644 of N₂O flux during winter thawing might be related to the rapid use of labile N made available during the soil freezing
645 period. Release of N₂O accumulated in the frozen soil might also explain some of the short-term N₂O flux peaks
646 during thaw (Maljanen et al., 2007; Pihlatie et al., 2010). The response of N₂O fluxes to soil thaw during winter was
647 weaker than the response especially to early winter soil freezing which highlights the importance of freezing-related
648 N₂O emissions in the studied ecosystem.

Commented [HR45]: Section about temporal variation and freeze-thaw cycles in the first version of the manuscript were combined. Results related to winter are also discussed.

Formatted: Highlight

649 soil and the tendency for high temporal variation of N₂O flux in several ecosystems (Maljanen et al., 2010;
650 Luo et al., 2012; Molodovskaya et al., 2012; Anthony and Silver, 2021), the complex temporal dynamics of N₂O
651 fluxes within and between years were expected. The high flux period starting conditions and modelling results support
652 previous evidence on the importance of freeze-thaw and dry-wet cycles strongly impacting temporal variation of N₂O
653 fluxes (Butterbach-Bahl et al., 2013; Risk et al., 2013; Wagner-Riddle et al., 2017; Congreves et al., 2018). However,
654 when comparing the temporal dynamics of N₂O flux with those previously published from boreal and temperate
655 regions (Maljanen et al., 2010; Pihlatie et al., 2010; Luo et al., 2012; Molodovskaya et al., 2012; Anthony and Silver,
656 2021; Gerin et al., 2023), the present data underline the importance of summer and winter N₂O fluxes contributing to
657 the annual N₂O budget more than fluxes in spring. Previously, several studies on both peat and mineral soils have
658 emphasized the importance of thaw-related spring N₂O fluxes in the annual N₂O budgets, with pronounced spring
659 N₂O fluxes in the annual N₂O budget, with distinct spring N₂O peaks in some cases accounting for a large fraction
660 of the annual budget (Pihlatie et al., 2010; Luo et al., 2012; Wang et al., 2023). In the present study, spring soil thaw
661 triggered N₂O emissions, but emissions increased slowly with increasing soil temperature and peaked in late spring or
662 summer, significantly later after soil thaw than reported in previous studies (Fig. 6 and S5). The strong temperature
663 dependence of spring N₂O fluxes may indicate that the substrate for the spring N₂O production comes from the
664 decomposing peat and litter in the warming soil. Temperature dependence of spring fluxes could be related to drained
665 peat soil, where the major source of N is known to be decomposing peat (Martikainen et al., 1993). Different responses
666 to thawing in winter compared to spring might be related to decreasing availability of N from early winter towards
667 spring (Koponen and Martikainen, 2004; Congreves et al., 2018), which also likely explains the tendency for stronger
668 response to freeze-thaw cycles in early winter. Only moderately high N₂O flux peaks were measured in spring and
669 early spring N₂O peaks were not typical. Year to year variation in N₂O budgets was more attributed to variation in
670 winter and summer N₂O fluxes than variation in spring N₂O fluxes.

671 During winters with discontinuous and shallow snow cover combined with high temporal variation in air
672 temperature below and above zero (2015–2016 and 2016–2017), the N₂O fluxes were higher compared to the snowier
673 winters with more stable temperature conditions (2017–2018 and 2018–2019). The insulating properties of the thicker
674 snowpack may have prevented the soil from freezing to deeper depth, decreasing N₂O fluxes during winter (Maljanen
675 et al., 2009; Ruan and Robertson, 2017). Thicker snowpack combined with less variable air temperature conditions in
676 the last two winters of the study period have likely decreased the number of freeze-thaw cycles and decreased intensity
677 of them leading to smaller total N₂O flux during winter.

678 High-flux periods during the growing season, especially in the summer, during summers were
679 associated with precipitation events that increased soil moisture and raised WTL (Fig. 6, 7 and S5). WTL. These
680 high-flux period events increased the total N₂O budget of the rainy summers (2016 and 2017), whereas the while N₂O
681 budget in dry summer (2018) was low in the warm and dry summer 2018. Precipitation events may have increased
682 the number of anoxic microsites in the soil, favoring N₂O production also through denitrification (Congreves et al.,
683 2018). Fast (2019; Song et al., 2022). Active peat decomposition in the warm soil during the summer has likely
684 reduced also decreased oxygen availability in the soil and increased N availability from the mineralizing peat resulting
685 in leading to high N₂O flux emissions after summer rain events (Maljanen et al., 2003). Low surface soil moisture

Commented [HR46]: Spring N2O fluxes are discussed more.

Formatted: English (United States), Highlight

Commented [RH47]: Comma was added

Formatted: Highlight

Formatted: Body Text

Formatted

686 has likely limited N₂O fluxes production during drought, leading to small N₂O budgets in dry summer are likely
687 explained by low microbial activity and substrate availability in the dry soil (Borken and Matzner, 2009; Congreves
688 et al., 2018). Our results on summer and winter N₂O fluxes suggest that low N₂O fluxes during dry summers might
689 offset the effect of the increasing winter N₂O fluxes on annual N₂O budgets if dry summers become more frequent in
690 the warming climate. (2018; Harry et al., 2021).

Formatted

Commented [HR48]: Conclusions related to climate change are highlighted more than previously.

Formatted: Highlight

691 N₂O fluxes during Autumn and spring N₂O fluxes varied relatively little between years with different weather
692 conditions, indicating weaker sensitivity of spring and autumn were low and showed little year-N₂O fluxes-to-year
693 variability (Fig. 5, 6 and S5). Low seasonal weather conditions. N₂O fluxes during autumn N₂O emissions have been
694 low also been measured in part of the previous studies (Maljanen et al., 2003; Luo et al., 2012), although but Pihlatie
695 et al. (2007)(2007) and Alm et al. (1999) found increased autumn N₂O fluxes after litter fall in drained peatland forests.
696 The low contribution of autumn N₂O fluxes to annual emissions in the present study is probably explained by the more
697 nutrient-rich peat and the lower importance of N₂O production in the litter layer in the total N₂O production
698 (Martikainen et al., 1993; Pihlatie et al., 2007). The results indicate that the site-specific differences in the peat nutrient
699 availability forest sites. Site-specific differences could alter the contributions of different seasons to annual N₂O
700 budgets. High temporal variability of fluxes and greater sensitivity of N₂O fluxes to environmental conditions in
701 nutrient-rich peatland forests are likely to increase the and affect sensitivity of N₂O budgets to increasing variability
702 in seasonal differing conditions in different seasons.

Formatted: English (United States)

Formatted: English (United States)

Formatted: English (United States)

Formatted: English (United States)

Formatted: English (United States)

Formatted: English (United States)

703 As the changing climate changes, the typical weather conditions for each season are predicted to change. In
704 northern latitudes, winters are expected to become warmer and wetter, and summer droughts are expected to become
705 more frequent (Zhao and Dai, 2017; IPCC, 2021). The high year to year variability in N₂O fluxes, which was largely
706 attributed to variation in summer and winter weather conditions, may imply changes and increased variability in annual
707 N₂O budgets if weather patterns of these seasons change and the frequency of extreme weather events increases due
708 to climate change.

Formatted: English (United States)

Formatted: First Paragraph

710 4.2. Linkages to spatial variation

711 Lower Capturing temporal patterns of N₂O fluxes from the three low-flux chambers (maximum flux < 400
712 $\mu\text{g N}_2\text{O m}^{-2} \text{h}^{-1}$) allowed us to explore the linkages between the spatial and temporal patterns of N₂O fluxes across
713 different measurement years. Lower N₂O fluxes from three of the chambers compared to high N₂O fluxes (maximum
714 flux > 1100 $\mu\text{g N}_2\text{O m}^{-2} \text{h}^{-1}$) measured in the other three high-flux chambers demonstrate the often spatially variable
715 nature of N₂O flux even on a small scale within a few tens of meters (Groffman et al., 2009; Hénault et al., 2012;
716 Jungkunst et al., 2012).

Formatted: English (United States)

Formatted: English (United States)

Formatted: English (United States), Highlight

Commented [HR49]: The section was made more compact and less important parts of the text (e.g. repetitive parts, multiple regression results) were removed

Commented [HR50]: Reminder about the fluxes was added in parentheses

717 What was notable was that the spatial differences in N₂O fluxes between chambers were persistent across
718 years, different years. The mean and the maximum daily mean fluxes were consistently larger for the high flux
719 chambers (Chambers 1-3), although differences between chambers were smaller during the low flux year 2018 due
720 to a larger decrease in N₂O fluxes in high flux chambers compared to low flux chambers. Despite large temporal
721 variations in flux within and between years, the spatial patterns of N₂O flux remained throughout the measurement
722 period.

723 The persistence of spatial variation implies that spatial variation of N₂O flux is controlled by long-term
 724 controls that persist throughout years with different weather conditions. ~~The long-term controls could include, for~~
 725 ~~example, spatial variation in soil properties (e.g. pH, porosity, C and N content) or placement of plant roots that have~~
 726 ~~both been suggested to affect the spatial variation of N₂O fluxes even on a very small scale within the soil (Butterbach-~~
 727 ~~Bahl et al., 2002; Jungkunst et al., 2012; Kuzyakov and Blagodatskaya, 2015).~~ However, it must be noted that results
 728 regarding the causes of within-site spatial variation have been highly variable between different studies, and few
 729 studies have managed to explain spatial variation well (Ball et al., 2000; Butterbach-Bahl et al., 2002; Yanai et al.,
 730 2003; Giles et al., 2012; Jungkunst et al., 2012). The linkages between soil properties, vegetation and N₂O fluxes are
 731 complex, with interactions making the relations between the N₂O flux and soil system difficult to understand.

732 ~~The long-term controls could include, for example, spatial variation in soil properties (e.g. pH, bulk density,~~
 733 ~~availability of different forms of N) or placement of plant roots both of which have been suggested to influence the~~
 734 ~~spatial variation in N₂O fluxes even at very small scales within the soil (Butterbach-Bahl et al., 2002; Jungkunst et al.,~~
 735 ~~2012; Kuzyakov and Blagodatskaya, 2015).~~ In the present study, the high-flux chambers had fewer trees ~~nearby~~
 736 ~~near~~ them than low-flux chambers, and the distance to nearby trees was ~~greater~~ (Fig. 1, Table S1). ~~Tree roots~~
 737 ~~shorter in low-~~ flux chambers (Fig. 1, Table S1). This could indicate the importance of trees shaping the spatial patterns of peatland
 738 forest floor N₂O fluxes, similar as suggested by Butterbach-Bahl et al. (2002) in mineral soil forest. Trees may have
 739 ~~affected~~ ~~impacted~~ the availability of ~~different forms of~~ nitrogen through nitrogen uptake and nitrogen inputs to soil
 740 ~~above and below ground~~ (Kaiser et al., 2011; Kuzyakov and Blagodatskaya, 2015; Hu et al., 2016), ~~resulting in higher~~
 741 ~~fluxes further away from the trees in this case. Because~~ ~~Since~~ ~~trees also affect the forest floor microclimate,~~ ~~ground~~
 742 ~~vegetation~~ and soil conditions ~~through~~ ~~by shading and affecting~~ ~~transpiration and by influencing the distribution of~~
 743 ~~rainfall and light~~ ~~rain fall~~ in the forest (Butterbach-Bahl et al., 2002; Aalto et al., 2022), variation in ~~the tree cover~~ ~~may~~
 744 ~~also~~ ~~could~~ have contributed to the spatio-temporal dynamics of peatland forest N₂O fluxes.

745 ~~Although the distance to trees seemed to explain some~~ chambers had persistently different levels ~~of the spatial~~
 746 ~~variation in N₂O flux,~~ throughout the study period, the chambers had clear similarities in the temporal dynamics of
 747 the N₂O flux (Fig. 4). High flux and baseline flux periods identified for each chamber occurred often at ~~the spatial~~
 748 ~~variation~~ ~~same time.~~ N₂O flux time series, especially ~~within the small and~~ ~~among high-flux and small flux chamber~~
 749 ~~groups, remained unexplained.~~ Ground vegetation was also not linked to spatial variation of N₂O. The results
 750 emphasize the importance of comprehensive soil sampling (e.g. N forms, bulk density, pH, C:N, root density) and
 751 chamber-specific measurements of environmental variables (e.g. soil moisture, soil temperature, WTL), when
 752 studying spatio-temporal variation of N₂O flux, especially in the forested study sites ~~unrelated,~~ ~~implying shared~~
 753 ~~temporal patterns but stronger similarities between chambers with variable microclimate.~~

754 ~~Despite the large spatial variation in the N₂O flux,~~ the high-flux periods identified for each chamber typically
 755 occurred at similar times, although the exact length and timing of the high-flux periods varied (Fig. 4, Table S4). ~~a~~
 756 ~~more similar flux level.~~ Similarities in the temporal ~~variation of fluxes suggest that temporal flux patterns between the~~
 757 ~~chambers indicate that the~~ changes in the soil environmental conditions ~~affected~~ ~~affect~~ N₂O fluxes relatively similarly
 758 across space. ~~In previous~~ ~~despite the large spatial variation in flux.~~

Formatted: Highlight

Field Code Changed

Field Code Changed

Formatted: Highlight

Commented [HR51]: Examples about possible soil properties that might control spatial variation were added

Field Code Changed

Field Code Changed

Commented [HR52]: Microclimate aspect was added

Formatted: Highlight

Formatted: Highlight

Formatted: Highlight

Formatted: Highlight

Formatted: Highlight

Formatted: Highlight

Formatted: Highlight

Formatted: Highlight

Formatted: Highlight

Formatted: Highlight

Formatted: Highlight

Formatted: English (United States), Highlight

Formatted: English (United States), Highlight

Formatted: Highlight

Formatted: English (United States), Highlight

Formatted: English (United States), Highlight

Formatted: English (United States), Highlight

Formatted: English (United States), Highlight

Formatted: English (United States), Highlight

Formatted: English (United States), Highlight

Commented [HR53]: Examples about possible soil properties that might be important to measure were added

Formatted: English (United States)

759 Previous studies, temporal using manual chambers in agricultural settings with more variable soil conditions
760 have found partly opposing results. Temporal patterns within sites were either variable or common shared
761 across space (Velthof et al., 2000; Krichels and Yang et al., 2019), with both findings mainly attributed to the spatio-
762 temporal variation of soil moisture. Stronger similarities in the temporal variation of N₂O flux within the low and
763 high-flux chamber groups indicate that some differences in the response of N₂O flux to environmental conditions
764 conditions. Soil moisture data from the individual chambers were not available here, but the chambers seemingly
765 reached soil conditions triggering N₂O production at similar times, although the resulting N₂O flux level varied
766 between chambers. In the presence of more topographical variation as in the study by Krichels et al. (2019), spatial
767 variation in soil conditions could have led to more variable temporal patterns in N₂O flux across space if triggering
768 conditions of N₂O production were reached at different times in different parts of the area. In the present study area,
769 the factors causing the high and temporally persistent spatial variation in flux have not affected the way fluxes respond
770 to temporal variation in soil conditions leading to similarities in temporal dynamics of the flux.

771 Differences in the temporal patterns between the high flux and low flux chambers were mainly related to the
772 length and relative height of the high flux periods as well as to the exact timing of the peak top within the high flux
773 periods. This has likely decreased the correlation of the temporal flux patterns between high flux chambers and low
774 flux chambers. Since soil temperature variables were able to explain differences in temporal patterns of N₂O flux
775 between most chamber pairs, N₂O peak length, timing, and relative height of flux peaks could be further shaped by
776 spatial differences in the magnitude by which N₂O fluxes respond to temperature conditions.

777 **4.3. Freeze-thaw cycles**

779 Increased winter N₂O fluxes occurred in different phases of freeze-thaw cycles; during the onset of freezing
780 periods, during repeated freeze-thaw events in the middle of the winter and during or after thawing in late winter and
781 spring. Increased N₂O fluxes in different phases of freeze-thaw periods can be seen, for example, in winter 2016–2017
782 (Fig. 6), with increased N₂O fluxes measured during the early winter freezing as well as during and after part of the
783 short freezing periods later in winter and spring.

784 Previous results about the timing of increased N₂O fluxes regarding freeze-thaw cycles have been variable.
785 Some studies report increased N₂O fluxes during the freezing period (Papen and Butterbach-Bahl, 1999; Teepe et al.,
786 2001; Maljanen et al., 2009, 2010; Ruan and Roberston, 2017), while part of the studies report high fluxes mainly
787 during and after the thawing (Koponen and Martikainen, 2004; Pihlatie et al., 2010; Luo et al., 2012; Molodovskaya
788 et al., 2012). Although here, the spring thaw resulted in a steady increase in N₂O flux, with peak N₂O flux reached
789 later in spring or early summer, short-term N₂O flux peak during soil melting was not observed. High variability in
790 the temporal patterns of winter and spring N₂O flux in different studies highlights the need to understand the causes
791 of site-specific differences that create variable winter N₂O flux patterns.

792 The highest winter N₂O fluxes typically occurred in the early winter soon after the soil freezing at the time
793 when frost reached 5 cm depth (Fig. 6 and 7, S5). Winter high flux periods with peak N₂O fluxes clearly elevated
794 from the baseline flux level were generally only measured during winters when soil frost reached 5 cm depth several
795 times (winters 2015–2016 and 2016–2017) and only during freeze-thaw cycles occurring at 5 cm depth (late winter

796 2016–2017). The importance of deeper soil freezing rather than freezing only of the soil surface may indicate that the
797 winter N₂O fluxes during freezing may be related to the overall spatial variation of the flux have originated from the
798 freezing peat rather than from the freezing litter at the surface of the soil. The importance of the severity of ground
799 frost and frost depth affecting N₂O fluxes has also been suggested by others (Nielsen et al., 2001; Koponen and
800 Martikainen, 2004; Luo et al., 2012). The conclusion about the possible source of winter N₂O fluxes in the topsoil
801 peat rather than in the soil surface litter differs from the results of Pihlatie et al. (2010) in a nutrient-poor peatland
802 forest site. More nutrient rich peat with a low C:N ratio may have favored N₂O production in peat (Regina et al., 1998;
803 Ojanen et al., 2010). Higher nitrogen availability in peat may have enabled a stronger link between winter N₂O fluxes
804 and conditions experienced in the peat. Site-specific differences in nutrient availability in different parts of the soil
805 may affect the sensitivity of winter N₂O fluxes to frost depth.

806
807 **4.34 Delayed responses and interactions**

808 The results of this study indicate that N₂O flux has a delayed response to precipitation events with peak N₂O
809 fluxes measured on average 4 days after general importance of lagged soil moisture and WTL peaks, and 5 conditions
810 affecting N₂O fluxes on the short time scale of 1–7 days. Peak N₂O fluxes were reached sometimes several days after
811 rainfall (Fig. the highest surface soil moisture and WTL values were measured (Fig. 9 and S7–S6). Studies mostly
812 conducted on from mineral soils in laboratories have found short time lags from the onset of anaerobiosis or water
813 saturation to the highest measured N₂O production, with or lags ranging from a few hours to less than between the
814 soil moisture peak and the highest N₂O fluxes, while others have found lags of a maximum of two days (Firestone and
815 Tiedje, 1979; Smith and Tiedje, 1979; Firestone and Tiedje, 1979; Smith and Tiedje, 1979; Russow et al., 2000; Song
816 et al., 2019). Compared to the previous studies, the observed Song et al., 2022). In this study, the lag times are long,
817 with indication time between surface soil moisture peak and the peak N₂O fluxes was typically at least two days, with
818 indications for even longer lags than seven days in some chambers.

819 The present data only allow us to hypothesize the causes of the long lag times after precipitation events. The
820 Long delays between the soil moisture peak and peak N₂O fluxes may be due to the ability of peat to retain moisture
821 and thus therefore retain anaerobic microsites in the soil means that anaerobic conditions soil for denitrification are
822 maintained and the possible co-occurrence of nitrification and denitrification can last for a longer than in time
823 compared to most mineral soils (Päivänen, 1973; Wrage et al., 2001; Walczak et al., 2002). The highest N₂O fluxes
824 during the growing season were reached on intermediate soil moisture (0.3–0.4 m⁻³ m⁻³) after the soil had started to
825 drain and WTL had started to decrease after a precipitation event (Fig. 7 and 9, S7). Based on this study and previous
826 laboratory studies, we suggest that after a period of high N₂O reduction activity and therefore relatively low N₂O
827 fluxes from denitrification in the wet soil soon after rain, N₂O production in the draining soil increased (Firestone and
828 Tiedje, 1979; Russow et al., 2000; Congreves et al., 2018). As soil continued to drain, conditions for simultaneous
829 nitrification and denitrification became optimal (Bateman and Baggs, 2005; Wang et al., 2021; Song et al., 2022),
830 further increasing N₂O production and leading to the peak N₂O flux some days after rain. The ability of peat to retain
831 moisture could extend the time for soil drainage after rainfall and thus time before optimal conditions for N₂O
832 production are reached. Hydrophobic properties of dry peat soils can also extend the time before N₂O fluxes respond

Formatted: Indent: First line: 0 cm
Commented [HR54]: Lags related to soil moisture are now discussed more carefully and uncertainties related to soil moisture data are brought up more. WTL and precipitation strengthens the discussion related to soil moisture more than previously.

Formatted: Highlight
Formatted: Highlight
Formatted: Highlight
Formatted: Highlight
Formatted: Highlight
Formatted: Highlight
Formatted: Highlight
Formatted: Highlight
Formatted: Highlight
Formatted: Highlight
Commented [HR55]: Explanation about the linkage between peat soil properties and long lag-times is now explained better and more clearly.

833 to soil wetting (Borken and Matzner, 2009) contributing to longer lag times. To determine exact lag times in response
834 to soil moisture peaks, chamber-specific soil moisture data would be required.

Formatted: Highlight

835 Differences in the importance of different variables and their lags between chambers may indicate varying
836 lag times and sensitivities to different soil moisture and WTL conditions across space. Despite spatial differences in
837 lag times and differences in the most important variables for which the lags were identified, the highest N₂O fluxes
838 on unfrozen soil were reached on intermediate soil moistures (0.3–0.4 m³·m⁻³) after the soil had started to drain and
839 WTL started to decrease after a precipitation event. The optimal conditions for high N₂O fluxes on intermediate soil
840 moistures could be explained by the simultaneous occurrence of oxic and anoxic soil microsites that allow
841 simultaneous nitrification and denitrification in draining soil (Bateman and Baggs, 2005; Wang et al., 2021; Song et
842 al., 2022).

843 Although models were not run for different seasons separately, the response of N₂O fluxes to precipitation
844 events seemed to be soil moisture peaks was slower during autumn and resulted in lower lag times between peak
845 N₂O fluxes and soil moisture peak increased and the height of the N₂O flux peaks (Fig. 6 and S5), decreased from
846 summer towards late autumn. Lower temperatures in autumn likely leading to decreased microbial activity and
847 mineralization decreasing availability of N from decomposing peat, which could in colder soil may explain lower
848 fluxes and slows response of N₂O fluxes to precipitation events soil moisture peaks in autumn (Holtan-Hartwig
849 et al., 2002). Chamber differences in the lag times associated with precipitation events and differences in the variable
850 importance of different environmental variables (Fig. 8 and S6) may also indicate varying sensitivities of N₂O
851 production to spatially varying soil conditions. These differences may be related to different microbial community,
852 substrate availability or soil properties that have been identified as important controls of N₂O production (Hénault et
853 al., 2012; Butterbach-Bahl et al., 2013; Hu et al., 2015) and are likely to shape the response of N₂O production to
854 environmental conditions. The finding reminds us of the importance of interactions affecting seasonal patterns of N₂O
855 fluxes.

Formatted: Highlight

857 5. Conclusions

858 This study shows extremely high temporal and spatial variability in peatland forest N₂O fluxes with
859 persistent spatial patterns across years with different environmental conditions, and common temporal dynamics across
860 space. The considerable small-scale spatial variation in N₂O fluxes was persistent in time and is therefore likely to be
861 influenced by relatively long-term controls in the soil. The temporal variation of N₂O flux was instead strongly
862 influenced by seasonal weather conditions, especially such as precipitation, snow depth and drought. Temporally
863 varying soil environmental conditions affect N₂O fluxes through complex responses that include delayed responses to
864 soil wetting. Interactions between spatially and temporally varying soil conditions, such as and interactions, leading
865 to high temporal variation in N₂O flux between years as well as within and between seasons. Responses of N₂O fluxes
866 to environmental conditions include time lags that further shape temporal patterns of N₂O fluxes.

867 The observed high peatland forest N₂O emissions highlight the role of N₂O emissions originating from non-
868 agricultural systems and the importance of considering the spatio-temporal dynamics of highly seasonally variable
869 N₂O fluxes, especially in boreal regions with strong seasonal patterns. The results indicate high importance of summer

Commented [HR56]: Conclusions section was updated. Main points highlighted in the discussion are now brought up also in the conclusions with stronger weight on conclusions related to changing climate.

Formatted: Highlight

Formatted: Highlight

Formatted: English (United States), Highlight

Formatted: Highlight

Formatted: Highlight

Formatted: Highlight

Formatted: Highlight

Formatted: Highlight

870 precipitation and winter temperature, further shape the spatio-temporal patterns of N₂O flux. The considerable small-
871 scale spatial variation in N₂O fluxes is likely to be influenced by relatively long-term controls such as soil properties
872 and positioning of trees and snow conditions for seasonal and annual N₂O budgets, and thus the possibility of increased
873 annual variability in N₂O emissions as seasonal weather conditions change in a warming climate.

Formatted: Highlight

874 The observed high N₂O fluxes from the peatland forest highlight the role of nutrient-rich drained peat soils
875 as hotspots for N₂O emissions in the boreal region. The dependence of N₂O budgets on seasonally varying weather
876 conditions suggests high sensitivity of peatland forest N₂O budgets to changing climate. Winter N₂O emissions will
877 likely increase in the future due to warming winters with shallow and discontinuous snow cover. Summer N₂O
878 emissions may decrease and possibly offset the effect of warming winters on annual N₂O budgets in dry years. Year-
879 to-year variation in N₂O emissions will likely increase as extreme weather events are predicted to become more
880 frequent.

Formatted: Highlight

882 6. Appendices

883 Appendix A. Thermal seasons

884 Thermal winter was the season with daily mean air temperatures persistently below 0 °C and thermal summer
885 a season with daily mean air temperatures persistently above 10 °C (Ruosteenoja et al., 2016; Finnish
886 Meteorological Institute, 2023). During spring and autumn, temperatures varied between 0–10 °C. Cumulative
887 temperature sums of daily mean temperatures were then used to identify the starting days of the thermal seasons at
888 which temperature went persistently above or below the seasonal temperature threshold (0 or 10 °C). The starting
889 day of the thermal winter was the day after the annual cumulative temperature sum reached the maximum. The starting
890 day of the thermal spring was the day after the minimum cumulative temperature sum was reached. Starting days of
891 thermal summer and autumn were calculated similarly but by extracting 10 °C from the air temperatures before
892 calculating the cumulative temperature sum (modified temperature sum). The day after the minimum modified
893 temperature sum was reached was defined as the starting date of the summer, while the maximum modified cumulative
894 temperature pointed the onset of thermal autumn.

896 Appendix B. Evaluating the model performance

897 R₂ of the chamber-specific models used in the analyses varied between 0.72 and 0.85 in OOB data, and
898 between 0.60 and 0.69 in training period evaluation data (30 % of training period data) (Table B1). When predicting
899 N₂O fluxes outside the training period (fourth measurement year), R₂ varied between 0.02 and 0.69. The
900 performance of N₂O gap-filling models was tested only using OOB data and evaluation data within the
901 whole study measurement period (30 % of data). For gap-filling models, R₂ in OOB data varied between 0.71 and 0.84,
902 while R₂ in evaluation data varied between 0.67 and 0.78 (Table B2).

903 For the models used in the analysis, the poor prediction accuracy outside of the training period, especially in
904 Chamber Chambers 3, 4, and 6, was likely due to overestimation of the general flux level during the relatively dry
905 year 2019, which was excluded from the training period (Fig. S9, S8). The model was also unable to predict anomalous

906 high-flux period in low-flux winter 2018–2019 in Chamber 5 likely due to a lack of chamber-specific soil temperature
 907 data deeper in the soil. The temporal patterns of the flux otherwise followed temporal patterns of measured fluxes
 908 relatively well. Poor prediction accuracy outside the training period in part of the chambers indicates that predicting
 909 N₂O fluxes to a year with distinct environmental conditions compared to the years in the training data may lead to
 910 large under or overestimation of N₂O fluxes. The used models could benefit from additional explanatory variables,
 911 such as redox potential or [the](#) availability of different forms of nitrogen (Rubol et al., 2012; Saha et al., 2020).
 912 Including additional soil variables in the model could decrease the need to have excessively large model training
 913 periods to accurately predict and gap-fill N₂O fluxes.

914

915 **Table B1: Model performance in evaluation datasets. Out-of-bag (OOB) data refers to data left outside**
 916 **model training in [randomRandom](#) forest with conditional inference trees, evaluation data within [the](#) training**
 917 **period refers to 30 % of data randomly left aside for model evaluation and evaluation data outside [the](#) training**
 918 **period refers to the fourth measurement year outside model training period [\(3 years\)](#).**
 919

Chamber	Evaluation data	RMSE	R ²
1	OOB	138.8	0.75
	Within training period	134.9	0.60
	Outside training period	113.7	0.67
2	OOB	105.7	0.84
	Within training period	106.0	0.69
	Outside training period	85.1	0.69
3	OOB	81.0	0.72
	Within training period	93.7	0.64
	Outside training period	75.7	0.02
4	OOB	36.3	0.83
	Within training period	29.5	0.77
	Outside training period	56.6	0.01
5	OOB	14.5	0.85
	Within training period	12.7	0.65
	Outside training period	22.0	0.33
6	OOB	10.2	0.85
	Within training period	10.3	0.68
	Outside training period	17.0	0.03

920

921 **Table B2: Performance of gap-filling models on evaluation datasets. Out-of-bag (OOB) data refers to data**
 922 **left outside model training in [randomRandom](#) forest with conditional inference trees and evaluation data**
 923 **within [the](#) training period refers to 30 % of training period data that was randomly left aside for model**
 924 **evaluation. [The training](#) Training period of gap-filling models covers the total [study](#) measurement period (4.5**
 925 **years).**
 926

Chamber	Evaluation data	RMSE	R ²
1	OOB	118.3	0.80
	Within training period	124.7	0.67
2	OOB	90.2	0.84
	Within training period	86.6	0.78
3	OOB	80.7	0.74
	Within training period	62.1	0.69
4	OOB	30.3	0.83
	Within training period	28.6	0.76
5	OOB	16.7	0.71
	Within training period	14.0	0.71
6	OOB	9.9	0.82
	Within training period	9.7	0.72

927
928
929
930
931
932
933
934
935
936
937
938
939
940
941
942
943
944
945
946
947

7. Data availability

Flux data and supporting environmental data are available at: <https://doi.org/10.5281/zenodo.8142188> (Rautakoski et al., 2023a). [Simplified R code of the machine learning part of the study is made freely available at: https://github.com/helenemilii/N2O_modeling](https://github.com/helenemilii/N2O_modeling). [R-codes used in data analysis are available from the corresponding author by request.](#) Python codes used in flux calculation and R codes used in data analysis are available from the corresponding author by request.

8. Supplement

The supplement of the article is available at: <https://doi.org/10.5281/zenodo.10533480> (Rautakoski et al., 2023b).

9. Author Contributions

AL, MA, MK and PO set up the study design. Field maintenance of measurement systems was carried out by MK, AL and PO. Fluxes were calculated by MK and filtered by HR. Data analysis, [modeling](#) and [writing of the article](#) ~~were done~~ [modelling was carried out](#) by HR with the support of AL and [other JM](#). ~~HR wrote the article with the help of~~ [co-authors](#).

10. Competing interests

The authors declare that they have no conflict of interest.

Formatted: Indent: First line: 0 cm

Commented [HR57]: Code of the machine learning part of the study was made available.

Commented [HR58]: Supplements were updated

948 **11. Acknowledgments**

949 We thank the Academy of Finland (Biogeochemical and biophysical feedbacks from forest harvesting to climate
950 change – BiBiFe, Grant no. 324259; Managing Forests for Climate Change Mitigation – FORCLIMATE, Grant no.
951 347794), and the Maj and Tor Nessling foundation (Grant no. 201700450) and [Wet Horizons \(Horizon Europe GAP-
952 101056848\)](#) for funding the work. We also thank for the support by the ACCC Flagship funded by the Academy of
953 Finland (Grant no. 337552) and the Ministry of Transport and Communications through the Integrated Carbon
954 Observation System (ICOS) and ICOS Finland. DeepL Write (DeepL SE, 2023) was used to improve the language of
955 the article.

956
957

Formatted: Font: 6 pt

958 **12. References**

- 959 Aalto, J., Tyystjärvi, V., Niittynen, P., Kemppinen, J., Rissanen, T., Gregow, H., and Luoto, M.: Microclimate
960 temperature variations from boreal forests to the tundra, *Agric. For. Meteorol.*, 323, 109037,
961 <https://doi.org/10.1016/j.agrformet.2022.109037>, 2022
- 962 Abd Elrahman, S. M., and Abraham, A.: A review of class imbalance problem. *J. Netw. Innov. Comput.*, 1, 332–
963 340, 2013
- 964 [Apley, D. W., and Zhu, J.: Visualizing the effects of predictor variables in black box supervised learning models.
965 *Journal of the Royal Statistical Society B: Stat. Methodol.*, 82\(4\), 1059–1086,
966 <https://doi.org/10.1111/rssb.12377>, 2020](#)
- 967 Alm, J., Saarnio, S., Nykänen, H., Silvola, J., and Martikainen, P.: Winter CO₂, CH₄ and N₂O fluxes on some natural
968 and drained boreal peatlands, *Biogeochemistry*, 44, 163–186, <https://doi.org/10.1007/BF00992977>, 1999
- 969 Anthony, T. L., and Silver, W. L.: Hot moments drive extreme nitrous oxide and methane emissions from
970 agricultural peatlands, *Glob. Global Change Biol.*, 27(20), 5141–5153, <https://doi.org/10.1111/gcb.15802>,
971 2021
- 972 Arnold, K. V., Weslien, P., Nilsson, M., Svensson, B. H., and Klemetsson, L.: Fluxes of CO₂, CH₄ and N₂O from
973 drained coniferous forests on organic soils, *For. Ecol. Manag.*, 210(1-3), 239–254,
974 <https://doi.org/10.1016/j.foreco.2005.02.031>, 2005
- 975 [Ball, B. C., Horgan, G. W., and Parker, J. P.: Short-range spatial variation of nitrous oxide fluxes in relation to
976 compaction and straw residues, *Eur. J. Soil Sci.*, 51\(4\), 607–616, \[https://doi.org/10.1046/j.1365-
2389.2000.00347.x\]\(https://doi.org/10.1046/j.1365-
977 2389.2000.00347.x\), 2000](#)
- 978 [Barrat, H. A., Evans, J., Chadwick, D. R., Clark, I. M., Le Coeq, K., and Cardenas, L.: The impact of drought and
979 rewetting on N₂O emissions from soil in temperate and Mediterranean climates, *Eur. J. Soil Sci.*, 72\(6\),
980 2504–2516, <https://doi.org/10.1111/ejss.13015>, 2021](#)
- 981 Barton, L., Wolf, B., Rowlings, D., Scheer, C., Kiese, R., Grace, P., Stefanova, K., and Butterbach-Bahl, K.:
982 Sampling frequency affects estimates of annual nitrous oxide fluxes, *Sci. Rep.*, 5(1), 15912,
983 <https://doi.org/10.1038/srep15912>, 2015

- 984 Bateman, E. J., and Baggs, E. M.: Contributions of nitrification and denitrification to N₂O emissions from soils at
 985 different water-filled pore space, *Biol. Fertil. Soils*, 41(6), 379–388, [https://doi.org/10.1007/s00374-005-](https://doi.org/10.1007/s00374-005-0858-3)
 986 0858-3, 2005
- 987 Bollmann, A., and Conrad, R.: Influence of O₂ availability on NO and N₂O release by nitrification and
 988 denitrification in soils, *Glob. Global Change Biol.*, 4(4), 387–396, [https://doi.org/10.1046/j.1365-](https://doi.org/10.1046/j.1365-2486.1998.00161.x)
 989 2486.1998.00161.x, 1998
- 990 Borken, W., and Matzner, E.: Reappraisal of drying and wetting effects on C and N mineralization and fluxes in
 991 soils, *Glob. Global Change Biol.*, 15(4), 808–824, <https://doi.org/10.1111/j.1365-2486.2008.01681.x>, 2009
- 992 Breiman, L.: Random forests, *Mach. Learn.*, 45, 5–32, <https://doi.org/10.1023/A:1010933404324>, 2001
- 993 Butlers, A., Lazdiņš, A., Kalēja, S., Purviņa, D., Spalva, G., Saule, G., and Bārdule, A.: CH₄ and N₂O emissions of
 994 undrained and drained nutrient-rich organic forest soil, *Forests*, 14(7), 1390,
 995 <https://doi.org/10.3390/f14071390>, 2023
- 996 Butterbach-Bahl, K., Rothe, A., and Papen, H.: Effect of tree distance on N₂O and CH₄ fluxes from soils in
 997 temperate forest ecosystems, *Plant Soil*, 240, 91–103, <https://doi.org/10.1023/A:1015828701885>, 2002
- 998 Butterbach-Bahl, K., Baggs, E. M., Dannemann, M., Kiese, R., and Zechmeister-Boltenstern, S.: Nitrous oxide
 999 emissions from soils: how well do we understand the processes and their controls?, *Philos. Trans. R. Soc.*
 1000 *Lond., B, Biol. Sci.*, 368(1621), 20130122, <https://doi.org/10.1098/rstb.2013.0122>, 2013
- 1001 Congreves, K. A., Wagner-Riddle, C., Si, B. C., and Clough, T. J.: Nitrous oxide emissions and biogeochemical
 1002 responses to soil freezing-thawing and drying-wetting, *Soil Biol. Biochem.*, 117, 5–1,
 1003 <https://doi.org/10.1016/j.soilbio.2017.10.040>, 2018
- 1004 Davidson, E. A., and Kanter, D.: Inventories and scenarios of nitrous oxide emissions, *Environ. Res. Lett.*, 9(10),
 1005 105012, <https://doi.org/10.1088/1748-9326/9/10/105012>, 2014
- 1006 Finnish Meteorological Institute: <https://en.ilmatieteenlaitos.fi/seasons-in-finland>, last access 11 July 2023
- 1007 Firestone, M., and Tiedje, J.: Temporal change in nitrous oxide and dinitrogen from denitrification following onset
 1008 of anaerobiosis, *Appl. Environ. Microbiol.*, 38(4), 673–679, [https://doi.org/10.1128/aem.38.4.673-](https://doi.org/10.1128/aem.38.4.673-679.1979)
 1009 679.1979, 1979
- 1010 [Forster, P., Storelvmo, T., Armour, K., Collins, W., Dufresne, J.-L., Frame, D., Lunt, D. J., Mauritsen, T., Palmer, M. D., Watanabe, M., Wild, M., and Zhang, H.: The Earth's Energy Budget, Climate Feedbacks, and Climate sensitivity. In *Climate Change 2021: The Physical Science Basis. Contribution of Working Group I to the Sixth Assessment Report of the Intergovernmental Panel on Climate Change*, edited by: Masson-Delmotte, V., Zhai, P., Pirani, A., Connors, S. L., Péan, C., Berger, S., Caud, N., Chen, Y., Goldfarb, L., Gomis, M. I., Huang, M., Leitzell, K., Lonnoy, E., Matthews, J. B. R., Maycock, T. K., Waterfield, T., Yelekçi, O., Yu, R., and Zhou, B., Cambridge University Press, Cambridge, United Kingdom and New York, NY, USA, pp. 923–1054, doi:10.1017/9781009157896.009, 2021](#)
- 1011
 1012
 1013
 1014
 1015
 1016
 1017
- 1018 Gerin, S., Vekuri, H., Liimatainen, M., Tuovinen, J.-P., Kekkonen, J., Kulmala, L., Laurila, T., Linkosalmi, M.,
 1019 Liski, J., Joki-Tokola, E., and Lohila, A.: Two contrasting years of continuous N₂O and CO₂ fluxes on a

Formatted: English (United States)

Formatted

Formatted: English (United States)

Formatted: English (United States)

Formatted: English (United States)

Formatted: English (United States)

Formatted: English (United States)

Formatted: English (United States)

1020 shallow-peated drained agricultural boreal peatland. *Agric. For. Meteorol.*, 341, 109630, SSRN [preprint],
 1021 <https://ssrn.com/abstract=4177973>, 1 August 2022

1022 Giles, M., Morley, N., Baggs, E. M., and Daniell, T. J.: Soil nitrate reducing processes—drivers, mechanisms for
 1023 spatial variation, and significance for nitrous oxide production. *Front. Microbiol.*, 3, 407,
 1024 <https://doi.org/10.1016/j.agrformet.2023.109630>, 2023 <https://doi.org/10.3389/fmicb.2012.00407>, 2012

1025 Giltrap, D. L., Berben, P., Palmada, T., and Saggarr, S.: Understanding and analysing spatial variability of nitrous
 1026 oxide emissions from a grazed pasture. *Agric. Ecosyst. Environ.*, 186, 1–10,
 1027 <https://doi.org/10.1016/j.agee.2014.01.012>, 2014

1028 Grace, P. R., Weerden, T. J., Rowlings, D. W., Scheer, C., Brunk, C., Kiese, R., Butterbach-Bahl, K., Rees, R. M.,
 1029 Robertson, G. P., and Skiba, U. M.: Global Research Alliance N₂O chamber methodology guidelines:
 1030 Considerations for automated flux measurement. *J. Environ. Qual.*, 49(5), 1126–1140,
 1031 <https://doi.org/10.1002/jeq2.20124>, 2020

1032 Groffman, P. M., Hardy, J. P., Driscoll, C. T., and Fahey, T. J.: Snow depth, soil freezing, and fluxes of carbon
 1033 dioxide, nitrous oxide and methane in a northern hardwood forest. *Glob. Change Biol.*, 12(9), 1748–1760,
 1034 <https://doi.org/10.1111/j.1365-2486.2006.01194.x>, 2006

1035 Groffman, P. M., Butterbach-Bahl, K., Fulweiler, R. W., Gold, A. J., Morse, J. L., Stander, E. K., Tague, C.,
 1036 Tonitto, C., and Vidon, P.: Challenges to incorporating spatially and temporally explicit phenomena
 1037 (hotspots and hot moments) in denitrification models. *Biogeochemistry*, 93(1-2), 49–77,
 1038 <https://doi.org/10.1007/s10533-008-9277-5>, 2009

1039 Hénault, C., Gossel, A., Mary, B., Roussel, M., and Léonard, J.: Nitrous oxide emission by agricultural soils: a
 1040 review of spatial and temporal variability for mitigation. *Pedosphere*, 22(4), 426–433,
 1041 [https://doi.org/10.1016/S1002-0160\(12\)60029-0](https://doi.org/10.1016/S1002-0160(12)60029-0), 2012

1042 Holtan-Hartwig, L., Dörsch, P., and Bakken, L. R.: Low temperature control of soil denitrifying communities:
 1043 kinetics of N₂O production and reduction. *Soil Biol. Biochem.*, 34(11), 1797–1806,
 1044 [https://doi.org/10.1016/S0038-0717\(02\)00169-4](https://doi.org/10.1016/S0038-0717(02)00169-4), 2002

1045 Hothorn, T., Hornik, K., and Zeileis, A.: Unbiased recursive partitioning: A Conditional inference framework. *J.*
 1046 *Comput. Graph. Stat.*, 15(3), 651–674, <https://doi.org/10.1198/106186006X133933>, 2006

1047 Hu, H. W., Chen, D., and He, J. Z.: Microbial regulation of terrestrial nitrous oxide formation: understanding the
 1048 biological pathways for prediction of emission rates. *FEMS Microbiol. Rev.*, 39(5), 729–749,
 1049 <https://doi.org/10.1093/femsre/fuv021>, 2015

1050 Hu, X., Liu, L., Zhu, B., Du, E., Hu, X., Li, P., Zhou, Z., Ji, C., Zhu, J., Shen, H., and Fang, J.: Asynchronous
 1051 responses of soil carbon dioxide, nitrous oxide emissions and net nitrogen mineralization to enhanced fine
 1052 root input. *Soil Biol. and Biochem.*, 92, 67–78, <http://dx.doi.org/10.1016/j.soilbio.2015.09.019>, 2016

1053 Huttunen, J. T., Nykänen, H., Martikainen, P. J., and Nieminen, M.: Fluxes of nitrous oxide and methane from
 1054 drained peatlands following forest clear-felling in southern Finland. *Plant Soil*, 255(2), 457–462,
 1055 <https://doi.org/10.1023/A:1026035427891>, 2003

Formatted: English (United States)

Formatted: English (United States)

Formatted: English (United States)

1056 IPCC: Summary for Policymakers, in: *Climate Change 2021: The Physical science basis. Contribution of working*
1057 *group I to the sixth assessment report of the Intergovernmental Panel on Climate Change*, edited by:
1058 *Masson-Delmotte, V., Zhai, P., Pirani, A., Connors, S. L., Péan, C., Berger, S., Caud, N., Chen, Y.,*
1059 *Goldfarb L., Gomis, M. J., Huang, M., Leitzell, K., Lonnoy, E., Matthews, J. B. R., Maycock, T. K.,*
1060 *Waterfield, T., Yelekçi, O., Yu, R., and Zhou, B., Cambridge University Press, Cambridge, United*
1061 *Kingdom and New York, NY, USA, 3–32, <https://doi.org/10.1017/9781009157896.001>, 2021*

1062 Ju, X., and Zhang, C.: Nitrogen cycling and environmental impacts in upland agricultural soils in North China: A
1063 review, *J. Integr. Agric.*, 16(12), 2848–2862, [https://doi.org/10.1016/S2095-3119\(17\)61743-X](https://doi.org/10.1016/S2095-3119(17)61743-X), 2017

1064 Jungkunst, H. F., Bargsten, A., Timme, M., and Glatzel, S.: Spatial variability of nitrous oxide emissions in an
1065 unmanaged old-growth beech forest, *J. Plant. Nutr. Soil Sci.*, 175(5), 739–749,
1066 <https://doi.org/10.1002/jpln.201100412>, 2012

1067 Kaiser, C., Fuchslueger, L., Koranda, M., Gorfer, M., Stange, C. F., Kitzler, B., Rasche, F., Strauss, J., Sessitsch, A.,
1068 Zechmeister-Boltenstern, S., and Richter, A.: Plants control the seasonal dynamics of microbial N cycling
1069 in a beech forest soil by belowground C allocation, *Ecology*, 92(5), 1036–1051, [https://doi.org/10.1890/10-](https://doi.org/10.1890/10-1011.1)
1070 [1011.1](https://doi.org/10.1890/10-1011.1), 2011

1071 Klemedtsson, L., Von Arnold, K., Weslien, P., and Gundersen, P.: Soil CN ratio as a scalar parameter to predict
1072 nitrous oxide emissions, *Glob. Global Change Biol.*, 11(7), 1142–1147, [https://doi.org/10.1111/j.1365-](https://doi.org/10.1111/j.1365-2486.2005.00973.x)
1073 [2486.2005.00973.x](https://doi.org/10.1111/j.1365-2486.2005.00973.x), 2005

1074 Koponen, H. T., and Martikainen, P. J.: Soil water content and freezing temperature affect freeze–thaw related N₂O
1075 production in organic soil, *Nutr. Cycl. Agroecosystems*, 69, 213–219,
1076 <https://doi.org/10.1023/B:FRES.0000035172.37839.24>, 2004

1077 Korhonen, K. T., Ahola, A., Heikkinen, J., Henttonen, H. M., Hotanen, J. P., Ihalainen, A., Melin, M., Pitkänen, J.,
1078 Rätty, M., Sirviö, M., and Strandström, M.: Forests of Finland 2014–2018 and their development 1921–
1079 2018, *Silva Fenn.*, 55(5), 10662, <https://doi.org/10.14214/sf.10662>, 2021

1080 Korhokoski, M., Tuovinen, J. P., Aurela, M., Koskinen, M., Minkkinen, K., Ojanen, P., Penttilä, T., Rainne, J.,
1081 Laurila, T., and Lohila, A.: Methane exchange at the peatland forest floor – automatic chamber system
1082 exposes the dynamics of small fluxes, *Biogeosciences*, 14(7), 1947–1967, [https://doi.org/10.5194/bg-14-](https://doi.org/10.5194/bg-14-1947-2017)
1083 [1947-2017](https://doi.org/10.5194/bg-14-1947-2017), 2017

1084 Korhokoski, M., Tuovinen, J. P., Penttilä, T., Sarkkola, S., Ojanen, P., Minkkinen, K., Rainne, J., Laurila, T., and
1085 Lohila, A.: Greenhouse gas and energy fluxes in a boreal peatland forest after clear-cutting,
1086 *Biogeosciences*, 16(19), 3703–3723, <https://doi.org/10.5194/bg-16-3703-2019>, 2019

1087 Korhokoski, M., Ojanen, P., Penttilä, T., Minkkinen, K., Sarkkola, S., Rainne, J., Laurila, T., and Lohila, A.: Impact
1088 of partial harvest on CH₄ and N₂O balances of a drained boreal peatland forest, *Agric. For. Meteorol.*, 295,
1089 108168, <https://doi.org/10.1016/j.agrformet.2020.108168>, 2020

1090 Korhokoski, M., Ojanen, P., Tuovinen, J. P., Minkkinen, K., Nevalainen, O., Penttilä, T., Aurela, M., Laurila, T.,
1091 and Lohila, A.: Partial cutting of a boreal nutrient-rich peatland forest causes radically less short-term on-

Formatted: English (United States)

Formatted: English (United States)

1092 site CO₂ emissions than clear-cutting, *Agric. For. Meteorol.*, 332, 109361,
1093 <https://doi.org/10.1016/j.agrformet.2023.109361>, 2023

1094 Koskinen, M., Minkkinen, K., Ojanen, P., Kämäräinen, M., Laurila, T., and Lohila, A.: Measurements of CO₂
1095 exchange with an automated chamber system throughout the year: challenges in measuring night-time
1096 respiration on porous peat soil, *Biogeosciences*, 11(2), 347–363, <https://doi.org/10.5194/bg-11-347-2014>,
1097 2014

1098 Krichels, A. H., and Yang, W. H.: Dynamic controls on field-scale soil nitrous oxide hot spots and hot moments
1099 across a microtopographic gradient, *J. Geophys. Res. Biogeosci.*, 124(11), 3618–3634,
1100 <https://doi.org/10.1029/2019JG005224>, 2019

1101 Kuzyakov, Y., and Blagodatskaya, E.: Microbial hotspots and hot moments in soil: Concept & review, *Soil Biol.*
1102 *Biochem.*, 83, 184–199, <https://doi.org/10.1016/j.soilbio.2015.01.025>, 2015

1103 Laine, J., Silvola, J., Tolonen, K., Alm, J., Nykänen, H., Vasander, H., Sallantausta, T., Savolainen, I., Sinisalo, J., and
1104 Martikainen, P. J.: Effect of water-level drawdown on global climatic warming: Northern peatlands,
1105 *Ambio*, 25(3), 179–184, <http://www.jstor.org/stable/4314450>, 1996

1106 Leppelt, T., Dechow, R., Gebbert, S., Freibauer, A., Lohila, A., Augustin, J., Drösler, M., Fiedler, S., Glatzel, S.,
1107 Höper, H., Järveoja, J., Lærke, P. E., Maljanen, M., Mander, Ü., Mäkiranta, P., Minkkinen, K., Ojanen, P.,
1108 Regina, K., and Strömngren, M.: Nitrous oxide emission budgets and land-use-driven hotspots for organic
1109 soils in Europe, *Biogeosciences*, 11(23), 6595–6612, <https://doi.org/10.5194/bg-11-6595-2014>, 2014

1110 [Liaw, A., and Wiener, M.: Classification and Regression by randomForest. R News 2\(3\), 18–22, https://CRAN.R-](#)
1111 project.org/doc/Rnews/, 2002

1112 Lin, F., Zuo, H., Ma, X., and Ma, L.: Comprehensive assessment of nitrous oxide emissions and mitigation
1113 potentials across European peatlands, *Environ. Pollut.*, 301, 119041,
1114 <https://doi.org/10.1016/j.envpol.2022.119041>, 2022

1115 Luo, G. J., Brüggemann, N., Wolf, B., Gasche, R., Grote, R., and Butterbach-Bahl, K.: Decadal variability of soil
1116 CO₂, NO, N₂O and CH₄ fluxes at the Höglwald Forest, Germany, *Biogeosciences*, 9(5), 1741–1763,
1117 <https://doi.org/10.5194/bg-9-1741-2012>, 2012

1118 Maljanen, M., Liikanen, A., Silvola, J., and Martikainen, P. J.: Nitrous oxide emissions from boreal organic soil
1119 under different land-use, *Soil Biol. Biochem.*, 35(5), 689–700, [https://doi.org/10.1016/S0038-](https://doi.org/10.1016/S0038-0717(03)00085-3)
1120 [0717\(03\)00085-3](https://doi.org/10.1016/S0038-0717(03)00085-3), 2003

1121 [Maljanen, M., Kohonen, A. R., Virkajärvi, P., Hytönen, J., Öquist, M., Sparrman, T., and Martikainen, P. J.: Fluxes](#)
1122 [and Nitrous oxide production of N₂O, CO₂ and CH₄ in boreal agricultural soil during winter as affected](#)
1123 [by soils with variable organic matter content at low temperature – snow cover. *Tellus B: Chemical and*](#)
1124 [Physical Meteorology](#), 59(5), 853-859, <https://doi.org/10.1111/j.1600-0889.2007.00304.x>,
1125 [2007 manipulation experiment, *Biogeosciences*, 6\(11\), 2461–2473, https://doi.org/10.5194/bg-6-2461-2009,](#)
1126 [2009](#)

Formatted: English (United States)

Formatted: English (United States)

Formatted: English (United States)

Formatted: English (United States)

Formatted: English (United States)

Formatted: English (United States)

Formatted: English (United States)

1127 Maljanen, M., Hytönen, J., and Martikainen, P. J.: Cold-season nitrous oxide dynamics in a drained boreal peatland
 1128 differ depending on land-use practice, *Can. J. For. Res.*, 40(3), 565–572, <https://doi.org/10.1139/X10-004>,
 1129 2010

1130 Martikainen, P. J., Nykänen, H., Crill, P., and Silvola, J.: Effect of a lowered water table on nitrous oxide fluxes
 1131 from northern peatlands, *Nature*, 366(6450), 51–53, <https://doi.org/10.1038/366051a0>, 1993

1132 Minkinen, K., Ojanen, P., Koskinen, M., and Penttilä, T.: Nitrous oxide emissions of undrained, forestry-drained,
 1133 and rewetted boreal peatlands, *For. Ecol. Manag.*, 478, 118494,
 1134 <https://doi.org/10.1016/j.foreco.2020.118494>, 2020

1135 Molodovskaya, M., Singurindy, O., Richards, B. K., Warland, J., Johnson, M. S., and Steenhuis, T. S.: Temporal
 1136 variability of nitrous oxide from fertilized croplands: Hot moment analysis, *Soil Sci. Soc. Am. J.*, 76(5),
 1137 1728–1740, <https://doi.org/10.2136/sssaj2012.0039>, 2012

1138 ~~Myhre, G., Shindell, D., Bréon, F. M., Collins, W., Fuglestedt, J., Huang, J., Koch, D., Lamarque, J. F., Lee, D.,~~
 1139 ~~Mendoza, B., Nakajima, T., Robock, A., Stephens, G., Takemura, T., and Zhang, H.: Anthropogenic and~~
 1140 ~~natural radiative forcing, in: Climate Change 2013: The Physical science basis. Contribution of working~~
 1141 ~~group I to the fifth assessment report of the Intergovernmental Panel on Climate Change, edited by:~~
 1142 ~~Stocker, T.F., Qin, D., Plattner, G. K., Tignor, M., Allen, S. K., Boschung, J., Nauels, A., Xia, Y., Bex, V.~~
 1143 ~~and Midgley, P. M., Cambridge University Press, Cambridge, United Kingdom and New York, NY, USA,~~
 1144 ~~659–740, https://www.ipcc.ch/site/assets/uploads/2018/02/WG1AR5_Chapter08_FINAL.pdf, 2013~~

1145 ~~Mäkiranta, P., Laiho, R., Penttilä, T., and Minkinen, K.: The impact of logging residue on soil GHG fluxes in a~~
 1146 ~~drained peatland forest, *Soil Biol. Biochem.*, 48, 1–9, <https://doi.org/10.1016/j.soilbio.2012.01.005>, 2012~~

1147 Nielsen, C. B., Groffman, P. M., Hamburg, S. P., Driscoll, C. T., Fahey, T. J., and Hardy, J. P.: Freezing effects on
 1148 carbon and nitrogen cycling in northern hardwood forest soils, *Soil Sci. Soc. Am. J.*, 65(6), 1723–1730,
 1149 <https://doi.org/10.2136/sssaj2001.1723>, 2001

1150 ~~Nickerson, N.: Evaluating gas emission measurements using Minimum Detectable Flux (MDF). Eosense Inc.,~~
 1151 ~~Dartmouth, Nova Scotia, Canada, [https://eosense.com/wp-content/uploads/2019/11/Eosense-white-paper-](https://eosense.com/wp-content/uploads/2019/11/Eosense-white-paper-Minimum-Detectable-Flux.pdf)~~
 1152 ~~[Minimum-Detectable-Flux.pdf](https://eosense.com/wp-content/uploads/2019/11/Eosense-white-paper-Minimum-Detectable-Flux.pdf), 2016~~

1153 Ojanen, P., Minkinen, K., Alm, J., and Penttilä, T.: Soil–atmosphere CO₂, CH₄ and N₂O fluxes in boreal forestry-
 1154 drained peatlands, *For. Ecol. Manag.*, 260(3), 411–421, <https://doi.org/10.1016/j.foreco.2010.04.036>, 2010

1155 Olden, J. D., Lawler, J. J., and Poff, N. L.: Machine learning methods without tears: A primer for ecologists, *Q. Rev.*
 1156 *Biol.*, 83(2), 171–193, <https://doi.org/10.1086/587826>, 2008

1157 ~~Pavelka, M., Acosta, M., Kiese, R., Altimir, N., Brümmer, C., Crill, P., Darenova, E., Fub, R., Gielen, B., Graf, A.,~~
 1158 ~~Klemedtsson, L., Lohila, A., Longdoz, B., Lindroth, A., Nilsson, M., Marañón Jiménez, S., Merbold, L.,~~
 1159 ~~Montagnani, L., Pechl, M., Pihlatie, M., Pumpanen, J., Serrano Ortiz, P., Silvennoinen, H., Skiba, U.,~~
 1160 ~~Vestin, P., Weslien, P., Janous, D., and Kutsch, W.: Standardisation of chamber technique for CO₂, N₂O~~
 1161 ~~and CH₄ fluxes measurements from terrestrial ecosystems. *Int. Agrophys.* 32, 569–587,~~
 1162 ~~<https://doi.org/10.1515/intag-2017-0045>, 2018~~

1163 Päivänen, J.: Hydraulic conductivity and water retention in peat soils, *Acta Forestalia Fennica*, 129(1–70), 1973

Formatted: English (United States)

Formatted: English (United States)

- 1164 Papen, H., and Butterbach-Bahl, K.: A 3-year continuous record of nitrogen trace gas fluxes from untreated and
 1165 limed soil of a N-saturated spruce and beech forest ecosystem in Germany: I. N₂O emissions, *J. Geophys.*
 1166 *Res. Atmos.*, 104(D15), 18487–18503, <https://doi.org/10.1029/1999JD900293>, 1999
- 1167 Pärn, J., Verhoeven, J. T. A., Butterbach-Bahl, K., Dise, N. B., Ullah, S., Aasa, A., Egorov, S., Espenberg, M.,
 1168 Järveoja, J., Jauhainen, J., Kasak, K., Klemedtsson, L., Kull, A., Laggoun-Défarge, F., Lapshina, E. D.,
 1169 Lohila, A., Lõhmus, K., Maddison, M., Mitsch, W. J., ... Mander, Ü.: Nitrogen-rich organic soils under
 1170 warm well-drained conditions are global nitrous oxide emission hotspots, *Nat. Commun.*, 9(1), 1135,
 1171 <https://doi.org/10.1038/s41467-018-03540-1>, 2018
- 1172 Pihlatie, M., Pumpanen, J., Rinne, J., Ilvesniemi, H., Simojoki, A., Hari, P., and Vesala, T.: Gas concentration
 1173 driven fluxes of nitrous oxide and carbon dioxide in boreal forest soil, *Tellus B Chem. Phys. Meteorol.*,
 1174 59(3), 458–469, <https://doi.org/10.1111/j.1600-0889.2007.00278.x>, 2007
- 1175 Pihlatie, M., Kiese, R., Brüggemann, N., Butterbach-Bahl, K., Kieloaho, A.-J., Laurila, T., Lohila, A., Mammarella,
 1176 I., Minkinen, K., Penttilä, T., Schönborn, J., and Vesala, T.: Greenhouse gas fluxes in a drained peatland
 1177 forest during spring frost-thaw event, *Biogeosciences*, 7(5), 1715–1727, [https://doi.org/10.5194/bg-7-1715-](https://doi.org/10.5194/bg-7-1715-2010)
 1178 2010, 2010
- 1179 Rautakoski, H., Korriakoski, M., Aurela, M., Minkinen, K., Ojanen, P., and Lohila, A.: 4.5 years of peatland forest
 1180 N₂O flux data data measured using automatic chambers, *Zenodo*, <https://doi.org/10.5281/zenodo.8142188>,
 1181 2023a
- 1182 Rautakoski, H., Korriakoski, M., Aurela, M., Minkinen, K., Ojanen, P., and Lohila, A.: Supplementary material to
 1183 the article "Exploring temporal and spatial variation of nitrous oxide flux using several years of peatland
 1184 forest automatic chamber data", *Zenodo*, <https://doi.org/10.5281/zenodo.10533480>, 2023b
- 1185 R Core Team: R: A language and environment for statistical computing, R Foundation for Statistical Computing,
 1186 Vienna, Austria, <https://www.R-project.org/>, 2021
- 1187 Reay, D. S., Davidson, E. A., Smith, K. A., Smith, P., Melillo, J. M., Dentener, F., and Crutzen, P. J.: Global
 1188 agriculture and nitrous oxide emissions, *Nat. Clim. Chang.*, 2(6), 410–416,
 1189 <https://doi.org/10.1038/nclimate1458>, 2012
- 1190 Regina, K., Martikainen, P. J., and Silvola, J.: Mechanisms of N₂O and NO production in the soil profile of a
 1191 drained and forested peatland, as studied with acetylene, nitrapyrin and dimethyl ether, *Biol. Fertil. Soils*,
 1192 27(2), 205–210, <https://doi.org/10.1007/s003740050421>, 1998
- 1193 Risk, N., Snider, D., and Wagner-Riddle, C.: Mechanisms leading to enhanced soil nitrous oxide fluxes induced by
 1194 freeze–thaw cycles, *Can. J. Soil Sci.*, 93(4), 401–414, <https://doi.org/10.4141/cjss2012-071>, 2013
- 1195 Ruan, L., and Robertson, G. P.: Reduced snow cover increases wintertime nitrous oxide (N₂O) emissions from an
 1196 agricultural soil in the upper U.S. Midwest, *Ecosystems*, 20(5), 917–927, [https://doi.org/10.1007/s10021-](https://doi.org/10.1007/s10021-016-0077-9)
 1197 016-0077-9, 2017
- 1198 Rubol, S., Silver, W. L., and Bellin, A.: Hydrologic control on redox and nitrogen dynamics in a peatland soil, *Sci.*
 1199 *Total Environ.*, 432, 37–46, <https://doi.org/10.1016/j.scitotenv.2012.05.073>, 2012

Formatted: Default Paragraph Font, Font: (Default)
+Body (Calibri), 11 pt,

Formatted: English (United States)

Formatted: English (United States)

Formatted: English (United States)

Formatted: English (United States)

1200 Ruosteenoja, K., Räisänen, J., [Venäläinen, A.](#), and [Kämäräinen, M.](#): Projections for the duration and degree days of
1201 [the Pirinen, P.: Projected changes in thermal seasons and the growing season in Europe derived from](#)
1202 [CMIP5 model output, Finland, Int. J. Climatol., 36\(8\), 3039–3055. https://doi.org/10.1002/joc.4535,](#)
1203 [2016\), 1473–1487, https://doi.org/10.1002/joc.2171, 2011,](#)
1204 [Russow, R., Sich, I., and Neue, H. U.: The formation of the trace gases NO and N₂O in soils by the coupled](#)
1205 [processes of nitrification and denitrification: results of kinetic 15N tracer investigations. Chem. Glob.](#)
1206 [Change Sci., 2\(3–4\), 359–366. https://doi.org/10.1016/S1465-9972\(00\)00012-X, 2000](#)
1207 Saha, D., Basso, B., and Robertson, G. P.: Machine learning improves predictions of agricultural nitrous oxide
1208 (N₂O) emissions from intensively managed cropping systems, *Environ. Res. Lett.*, 16(2), 024004,
1209 <https://doi.org/10.1088/1748-9326/abd2f3>, 2021
1210 Shakoor, A., Shahzad, S. M., Chatterjee, N., Arif, M. S., Farooq, T. H., Altaf, M. M., Tufail, M. A., Dar, A. A., and
1211 Mehmood, T.: Nitrous oxide emission from agricultural soils: Application of animal manure or biochar? A
1212 global meta-analysis, *J. Environ. Manage.*, 285, 112170, <https://doi.org/10.1016/j.jenvman.2021.112170>,
1213 2021
1214 [Sharma, S., Szele, Z., Schilling, R., Munch, J. C., and Schloter, M.: Influence of freeze-thaw stress on the structure](#)
1215 [and function of microbial communities and denitrifying populations in soil. Appl. Environ. Microbiol.,](#)
1216 [72\(3\), 2148-2154. https://doi.org/10.1128/AEM.72.3.2148-2154.2006, 2006](#)
1217 Smith, M., and Tiedje, J.: Phases of denitrification following oxygen depletion in soil, *Soil Biol. Biochem.*, 11, 261–
1218 267, [https://doi.org/10.1016/0038-0717\(79\)90071-3](https://doi.org/10.1016/0038-0717(79)90071-3), 1979
1219 Song, X., Ju, X., Topp, C. F. E., and Rees, R. M.: Oxygen regulates nitrous oxide production directly in agricultural
1220 soils, *Environ. Sci. Technol.*, 53(21), 12539–12547, <https://doi.org/10.1021/acs.est.9b03089>, 2019
1221 Song, X., Wei, H., Rees, R. M., and Ju, X.: Soil oxygen depletion and corresponding nitrous oxide production at hot
1222 moments in an agricultural soil, *Environ. Pollut.*, 292, 118345,
1223 <https://doi.org/10.1016/j.envpol.2021.118345>, 2022
1224 Strobl, C., Boulesteix, A.-L., Zeileis, A., and Hothorn, T.: Bias in random forest variable importance measures:
1225 Illustrations, sources and a solution, *BMC Bioinform.*, 8(1), 25, <https://doi.org/10.1186/1471-2105-8-25>,
1226 2007
1227 Sutton, M. A., Nemitz, E., Erisman, J. W., Beier, C., Butterbach-Bahl, K., Cellier, P., de Vries, W., Cotrufo, F.,
1228 Skiba, U., Di Marco, C., Jones, S., Laville, P., Soussana, J. F., Loubet, B., Twigg, M., Famulari, D.,
1229 Whitehead, J., Gallagher, M. W., Nefel, A., Flechard, C. R., Herrmann, B., Calanca, P. L., Schjoerring, J.
1230 K., Daemmgen, U., Horvath, L., Tang, Y. S., Emmett B. A., Tietema A., Peñuelas, J., Kesik M.,
1231 Brueggemann, N., Pilegaard K., Vesala, T., Campbell, C. L., Olesen, J. E., Dragosits, U., Theobald, M. R.,
1232 Levy, P., Mobbs, D. C., Milne, R., Viovy, N., Vuichard, N., Smith, J. U., Smith, P., Bergamaschi, P.,
1233 Fowler, D., and Reis, S.: Challenges in quantifying biosphere–atmosphere exchange of nitrogen species,
1234 *Environ. Pollut.*, 150(1), 125–139, <https://doi.org/10.1016/j.envpol.2007.04.014>, 2007
1235 Teepe, R., Brumme, R., and Beese, F.: Nitrous oxide emissions from soil during freezing and thawing periods, *Soil*
1236 *Biol. Biochem.*, 33(9), 1269–1275, [https://doi.org/10.1016/S0038-0717\(01\)00084-0](https://doi.org/10.1016/S0038-0717(01)00084-0), 2001

Formatted: English (United States)

Formatted: English (United States)

Formatted: English (United States)

Formatted: English (United States)

Formatted: English (United States)

1237 Teepe, R., Vor, A., Beese, F., and Ludwig, B.: Emissions of N₂O from soils during cycles of freezing and thawing
1238 and the effects of soil water, texture and duration of freezing, *Eur. J. Soil Sci.*, 55(2), 357–365,
1239 <https://doi.org/10.1111/j.1365-2389.2004.00602.x>, 2004

1240 Thompson, R. L., Lassaletta, L., Patra, P. K., Wilson, C., Wells, K. C., Gressent, A., Koffi, E. N., Chipperfield, M.
1241 P., Winiwarter, W., Davidson, E. A., Tian, H., and Canadell, J. G.: Acceleration of global N₂O emissions
1242 seen from two decades of atmospheric inversion, *Nat. Clim. Chang.*, 9(12), 993–998,
1243 <https://doi.org/10.1038/s41558-019-0613-7>, 2019

1244 Tian, H., Yang, J., Lu, C., Xu, R., Canadell, J. G., Jackson, R. B., Arneeth, A., Chang, J., Chen, G., Ciais, P., Gerber,
1245 S., Ito, A., Huang, Y., Joos, F., Lienert, S., Messina, P., Olin, S., Pan, S., Peng, C., ... Zhu, Q.: The global
1246 N₂O model intercomparison project, *Bull. Am. Meteorol. Soc.*, 99(6), 1231–1251,
1247 <https://doi.org/10.1175/BAMS-D-17-0212.1>, 2018

1248 Tian, H., Xu, R., Canadell, J. G., Thompson, R. L., Winiwarter, W., Suntharalingam, P., Davidson, E. A., Ciais, P.,
1249 Jackson, R. B., Janssens-Maenhout, G., Prather, M. J., Regnier, P., Pan, N., Pan, S., Peters, G. P., Shi, H.,
1250 Tubiello, F. N., Zaehle, S., Zhou, F., ... Yao, Y.: A comprehensive quantification of global nitrous oxide
1251 sources and sinks, *Nature*, 586(7828), 248–256, <https://doi.org/10.1038/s41586-020-2780-0>, 2020

1252 Van Rossum, G., and Drake Jr, F. L.: Python tutorial, 620, Centrum voor Wiskunde en Informatica, Amsterdam,
1253 The Netherlands, 1995

1254 Velthof, G. L., Groenigen, J. W., Gebauer, G., Pietrzak, S., Jarvis, S. C., Pinto, M., Corré, W., and Oenema, O.:
1255 Temporal stability of spatial patterns of nitrous oxide fluxes from sloping grassland, *J. Environ. Qual.*,
1256 29(5), 1397–1407, <https://doi.org/10.2134/jeq2000.00472425002900050005x>, 2000

1257 Wagner-Riddle, C., Congreves, K. A., Abalos, D., Berg, A. A., Brown, S. E., Ambadan, J. T., Gao, X., and Tenuta,
1258 M.: Globally important nitrous oxide emissions from croplands induced by freeze–thaw cycles, *Nat.*
1259 *Geosci.*, 10(4), 279–283, <https://doi.org/10.1038/ngeo2907>, 2017

1260 Walczak, R., Rovdan, E., and Witkowska-Walczak, B.: Water retention characteristics of peat and sand mixtures,
1261 *Int. Agrophys.*, 16(2), 2002

1262 Wang, Q., Zhou, F., Shang, Z., Ciais, P., Winiwarter, W., Jackson, R. B., Tubiello, F. N., Janssens-Maenhout, G.,
1263 Tian, H., Cui, X., Canadell, J. G., Piao, S., and Tao, S.: Data-driven estimates of global nitrous oxide
1264 emissions from croplands, *Natl. Sci. Rev.*, 7(2), 441–452, <https://doi.org/10.1093/nsr/nwz087>, 2020

1265 Wang, C., Amon, B., Schulz, K., and Mehdi, B.: Factors that influence nitrous oxide emissions from agricultural
1266 soils as well as their representation in simulation models: A Review, *Agronomy*, 11(4), 770,
1267 <https://doi.org/10.3390/agronomy11040770>, 2021

1268 Wang, X., Wang, S., Yang, Y., Tian, H., Jetten, M. S. M., Song, C., and Zhu, G.: Hot moment of N₂O emissions in
1269 seasonally frozen peatlands, *J. ISME*, 1(1), 1–11, <https://doi.org/10.1038/s41396-023-01389-x>, 2023

1270 Wrage, N., Velthof, G. L., Beusichem, M. L. van, and Oenema, O.: Role of nitrifier denitrification in the production
1271 of nitrous oxide, *Soil Biol. Biochem.*, 33(12-13), 1723–1732, [https://doi.org/10.1016/S0038-](https://doi.org/10.1016/S0038-0717(01)00096-7)
1272 [0717\(01\)00096-7](https://doi.org/10.1016/S0038-0717(01)00096-7), 2001

1273 Wrage-Mönnig, N., Horn, M. A., Well, R., Müller, C., Velthof, G., and Oenema, O.: The role of nitrifier
1274 denitrification in the production of nitrous oxide revisited, *Soil Biol. Biochem.*, 33(12–13), 1723–1732,
1275 <https://doi.org/10.1016/j.soilbio.2018.03.020>, 2018

1276 Yanai, J., Sawamoto, T., Oe, T., Kusa, K., Yamakawa, K., Sakamoto, K., Naganawa, T., Inubushi, K., Hatano, R.,
1277 and Kosaki, T.: Spatial variability of nitrous oxide emissions and their soil-related determining factors in an
1278 agricultural field, *J. Environ. Qual.*, 32(6), 1965–1977, <https://doi.org/10.2134/jeq2003.1965>, 2003

1279 Zeileis, A., Hothorn, T., and Hornik, K.: Model-Based Recursive Partitioning, *J. Comput. Graph. Stat.*, 17(2), 492–
1280 514, <https://doi.org/10.1198/106186008X319331>, 2008

1281 [Zhao, T., and Dai, A.: Uncertainties in historical changes and future projections of drought. Part II: model simulated](#)
1282 [historical and future drought changes, *Clim. Change*, 144\(3\), 535–548, \[https://doi.org/10.1007/s10584-016-\]\(https://doi.org/10.1007/s10584-016-1742-x\)](#)
1283 [1742-x, 2017](#)

1284 Zhu, X., Burger, M., Doane, T. A., and Horwath, W. R.: Ammonia oxidation pathways and nitrifier denitrification
1285 are significant sources of N₂O and NO under low oxygen availability, *Proc. Natl. Acad. Sci. U.S.A.*,
1286 110(16), 6328–6333, <https://doi.org/10.1073/pnas.1219993110>, 2013

1287
1288